Research on Multi-objective Active Power Optimization Simulation of Novel Improved Whale Optimization Algorithm

Gonggui Chen, Xilai Zhao, Yi Xiang, Xianjun Zeng and Hongyu Long*

Abstract— **The Whale optimization algorithm (WOA) is adopted to solve the non-convex optimal power flow (OPF) problem in this paper. To balance the exploration and exploitation of standard WOA algorithm in solving the OPF problem, the multi-objective novel improved whale optimization algorithm (MONIWOA) is proposed. In the MONIWOA approach, the piecewise non-linear strategy and dual dynamic weights mode are applied to balance the global exploration and local development capabilities, the Lévy flight mechanism can increase the solutions' diversity with its random step pattern, which plays a vital role in the global exploration. Moreover, a constrains-prior Pareto-dominant rule (CPDR) strategy is proposed to ensure the non-violation of state variables' inequality constraints concurrently. To obtain better-distributed Pareto optimal solution sets (POS), a sorting method with crowding distance and rank strategy (CDRS) is adopted. What's more, an effective fuzzy sorting method is presented to obtain the best compromise solution (BCs) in solving multi-objective optimal power flow (MOOPF) problems. Eight test cases are carried on the standard IEEE 30-bus, IEEE 57-bus and IEEE 118-bus systems. The Pareto front sets (PFs) and BCs obtained by the MONIWOA are more superior to the ones of multi-objective Particle Swarm Optimization (MOPSO) and multi-objective Differential Evolution algorithm (MODE). Furthermore, the analyses of the obtained solutions using GD and SP show that the MONIWOA has significant advantages to gain more uniform distribution and better convergence.**

Index Terms— **multi-objective novel improved whale optimization algorithm; optimal power flow; constrains-prior Pareto-dominant rule; crowding distance and rank strategy**

Manuscript received April 13, 2021; revised August 7, 2021. This work was supported by the National Natural Science Foundation of China under Grant 51207064.

Gonggui Chen is a professor of Key Laboratory of Industrial Internet of Things and Networked Control, Ministry of Education, Chongqing University of Posts and Telecommunications, Chongqing 400065, China; Chongqing Key Laboratory of Complex Systems and Bionic Control, Chongqing University of Posts and Telecommunications, Chongqing 400065, China (e-mail: chenggpower@ 126.com).

Xilai Zhao is a master degree candidate of Chongqing Key Laboratory of Complex Systems and Bionic Control, Chongqing University of Posts and Telecommunications, Chongqing 400065, China (e-mail: S190301014@stu.cqupt.edu.cn).

Yi Xiang is a senior engineer of the Northwest Branch of State Grid Corporation of China, Xi'an 710048, China (e-mail:xiangy@nw.sgcc.com.cn).

Xianjun Zeng is a senior engineer of State Grid Chongqing Electric Power Company, Chongqing 400015, China (e-mail: 13594255525@139.com).

Hongyu Long is a professor level senior engineer of Chongqing Key Laboratory of Complex Systems and Bionic Control, Chongqing University of Posts and Telecommunications, Chongqing 400065, China(corresponding author to provide phone: +8613996108500; e-mail: longhongyu20@163.com).

I. Introduction

The concept of OPF is proposed by Carpentier in 1962 and the study of OPF has attracted the attention of scholars in the field of power system for many decades. The aim of OPF program is to achieve optimal distribution of the real power or the reactive power by satisfying equality and inequality physical constraints [1-5]. The optimizing of single-objective such as fuel cost, emission, real power loss or transmission loss can't meet the practical demands of users. Hence, the OPF problem has developed into a study of multi-objective optimal power flow (MOOPF) problem.

In the MOOPF problems, the optimizing process must consider more than one conflicting objectives, and all the various should own no violations of constraints concurrently. The highly constrained, large-scale and nonlinear MOOPF problem is to obtain the Pareto optimal solution set (POS) and get a best compromise solution (BCs) ultimately [6,7]. Over the recent years, a great number of intelligent algorithms have been applied to tackle the MOOPF problems successfully. Some intelligent algorithms like Gaussian bare-bones imperialist competitive algorithm [8], self-adaptive particle swarm optimization and differential evolution algorithms [9], multi-objective modified pigeon algorithm [10], evolutionary algorithm [11], and the differential search algorithm [12], are shown excellent performance when solving multi-objective problems.

Proposed in 2016, the whale optimization algorithm (WOA) is put forward by mimicking the hunting strategy of humpback whales [13]. The standard whale optimization algorithm owns competitive advantages in solving complex engineering problems and can get solutions of better accuracy when compared with many other meta-heuristic optimization algorithms. The WOA has been successfully adopted to solve the wind speed prediction problem [14], quadratic assignment problem [15], feature selection problem [16], data clustering problem [17], environment economic power dispatch problem [18], and multilevel thresholding image segmentation problem [19]. However, the basic whale optimization algorithm is easy to trap in local optima and premature convergence when dealing with MOOPF [20]. In order to overcome these weaknesses, this paper adopts the piecewise non-linear strategy, dual dynamic weights mode and Lévy flight mechanism to enhance the outperformance of the WOA algorithm. The piecewise non-linear strategy and dual dynamic weights mode are used to improve the exploration and exploitation, and the Lévy flight mechanism is used to improve the exploitation phase. In order to obtain high-quality POS sets and evenly-distributed Pareto fronts (PF), a sorting method with crowding-distance rank-calculation strategy (CDRS) and a constrains-prior Pareto-dominant rule (CPDR) are proposed in this paper. To verify the superiority and feasibility of aforementioned improvement strategies, a large number of simulation cases are executed in the IEEE 30-bus, IEEE 57-bus and IEEE 118-bus systems. In addition, the generational distance (GD) and spacing (SP) indicators are employed to calculate the stability and diversity. The simulation results and comprehensive analysis validate the better performance of the MONIWOA as compared to multi-objective Particle Swarm Optimization (MOPSO) and multi-objective Differential Evolution algorithm (MODE).

The rest of this paper is arranged as follows: Section II gives the mathematical model of MOOPF problems. Section III describes the basic WOA algorithm, the MONIWOA algorithm, the CPDR rule and the novel CDRS strategy. Section IV displays eight simulation results and comparisons with other algorithms. Eventually, Section V provides the summary of all the former contents.

II. Mathematical Model

Generally speaking, the aim of solving MOOPF problem is to optimize more than two objective and all the variables must satisfy several equality constraints and inequality constraints [21]. The mathematical model can be expressed as follows:

$$\min\ F_{ob}(x,u) = \min((f_1(x,u),\cdot\cdot, f_i(x,u),\cdot\cdot, f_M(x,u)) \quad (1)$$

Subject to:

$$E_h(x,u) = 0,\quad \mathrm{h} = 1,2,\cdots,\mathrm{k} \quad (2)$$

$$I_j(x,u) \le 0,\quad j = 1,2,\cdots,\mathrm{g} \quad (3)$$

where $f_i(x,u)$ represents the ith objective function and $M(M\ge 2)$ is the number of optimal objectives. The x indicates the state variables and u indicates the control variables. $E_h(x,u)$ indicate inequality constraints (ICs), $I_j(x,u)$ indicate equality constraints (ECs).

A. Objective functions

The aim of MOOPF research is to realize the best operating state of the power system by adjusting discrete and continuous control variables. The active power loss P_l, the basic fuel cost Fc, the emission Em, the fuel cost with value-point loadings F_v and the voltage stability index L_in, are involved in this paper.

1) minimization of P_l

$$\min P_l = \min \sum_{k=1}^{N_E} g_k (V_i^2 + V_j^2 - 2V_iV_j\cos\delta_{ij})\ MW \quad (4)$$

where N_E is the total number of branches. $g_{k(i,j)}$ is the conductance of the kth branch between node i and node j. V_i and V_j are the voltage magnitude of node i and node j. δ_{ij} represents the voltage angle between node i and node j.

2) minimization of Fc

$$\min F_c = \min \sum_{i=1}^{N_G} (a_i + b_i P_{Gi} + c_i P_{Gi}^2)\ \$/h \quad (5)$$

where a_i, b_i, c_i are the fuel cost coefficients of the ith generator. P_{Gi} is the active power of the ith generator. N_G indicates the amount of generators.

3) minimization of Em

$$\min E_m = \min \sum_{i=1}^{N_G} [\alpha_i P_{Gi}^2 + \beta_i P_{Gi} + \gamma_i + \eta_i \exp(\lambda_i P_{Gi})]\ ton/h \quad (6)$$

where α_i, β_i, γ_i, η_i and λ_i are the emission coefficients of the ith generator.

4) minimization of F_v

$$\min F_v = \min \sum_{i=1}^{N_G} (a_i + b_i P_{Gi} + c_i P_{Gi}^2 + \left| d_i \times \sin(e_i \times (P_{Gi}^{\min} - P_{Gi})) \right|)\ \$/h \quad (7)$$

where d_i and e_i are the fuel cost coefficients of the ith generator.

5) minimization of L_in

$$\min(L\text{-}in) = \min[\max(L_j)] \quad (8)$$

$$L_j = \left| 1 - \sum_{i=1}^{N_{PV}} F_{ji} \frac{V_i}{V_j} \right|,\quad j = 1,2,\cdots \mathrm{N}_{PQ} \quad (9)$$

where N_{PV} and N_{PQ} are the number of PV nodes and the number of PQ nodes. F_{ji} can be estimated from the Y bus matrix. V_i and V_j are the voltages of the ith PV node and the voltages of the jth PQ node.

B. Constraint strategies of MOOPF

The MOOPF problem is a highly constrained non-linear problem where all the variables must own no violations of ECs and ICs [22]. The best compromise solutions should meet all the ECs and ICs.

1) ECs

The ECs illustrate the relation of active and reactive power balance in the standard power system, which can be expressed as follows:

$$P_{Gi} - P_{Di} = V_i \sum_{j\in N_i} V_j (G_{ij}\cos\delta_{ij} + B_{ij}\sin\delta_{ij}), i \in N \quad (10)$$

$$Q_{Gi} - Q_{Di} = V_i \sum_{j\in N_i} V_j (G_{ij}\sin\delta_{ij} - B_{ij}\cos\delta_{ij}),\quad i \in N_{PQ} \quad (11)$$

where N_i is the number of nodes connected to node i (excluding node i). N is the number of system nodes but except the slack node. P_{Li} and Q_{Li} represent the active and reactive power of load node i. G_{ij} and B_{ij} are the mutual conductance and the mutual susceptance.

2) ICs

The ICs involve state variables and control variables, which are defined as follows.

a) state variables

- active power P_{Gref}

$$P_{G\mathrm{ref},\min} \le P_{G\mathrm{ref}} \le P_{G\mathrm{ref},\max} \quad (12)$$

- voltage limits

$$V_{Li,\min} \le V_{Li} \le V_{Li,\max},\ i \in N_{PQ} \quad (13)$$

- reactive power limits

$$Q_{Gi,\min} \le Q_{Gi} \le Q_{Gi,\max},\ i \in N_G \quad (14)$$

- apparent power flow limits of all branches

$$S_{ij} - S_{ij,\max} \le 0,\ ij \in N_L \quad (15)$$

b) control variables

- active output P_{Gi}

$$P_{Gi,\min} \le P_{Gi} \le P_{Gi,\max},\ i \in N_G \quad (16)$$

- generator terminal voltage V_{Gi}

$$V_{Gi,\min} \le V_{Gi} \le V_{Gi,\max},\ i \in N_G \quad (17)$$

- transformer tap-settings T_i

$$T_{i,\min} \le T_i \le T_{i,\max}, \ i \in N_T \tag{18}$$

- reactive power injection Q_C

$$Q_{Ci,\min} \le Q_{Ci} \le Q_{Ci,\max}, \ i \in N_C \tag{19}$$

where N_T and N_C indicate the amount of transformers and compensators.

III. MONIWOA FOR MOOPF PROBLEM

The basic whale optimization algorithm owns many drawbacks which make the optimization of MOOPF problems inefficient. The novel improved WOA algorithm is proposed to overcome drawbacks and improve the efficiency and accuracy of solving the Multi-objective optimal constrained MOOPF problems.

A. Overview of the basic WOA

The whale optimization algorithm is a new meta-heuristic algorithm inspired by imitating the hunting behavior of humpback whales [13]. The basic WOA algorithm completes the foraging process through three operators: encircling prey, spiral bubble-net attacking and searching for prey randomly. The mathematical model of WOA algorithm is described as follows:

1) Encircling prey strategy

In this phase, the prey represents the best candidate solution. The best candidate solution will be updated in each iteration and humpback whales can update their location according to the best candidate solution. This behavior can be modeled as follows:

$$D = | C \times X_{best}(t) - X(t) | \tag{20}$$

$$X(t+1) = X_{best}(t) - A \times D \tag{21}$$

$$A = 2a \times r_1 - a \tag{22}$$

$$C = 2 \times r_2 \tag{23}$$

where t indicates the current iteration. $X(t)$ represents the current position of the humpback whales. $X_{best}(t)$ represents the best candidate acquired in the current iteration. A and C are auxiliary coefficient vectors. r_1 and r_2 are random numbers in [0,1], a is a constant which is linearly decreasing from 2 to 0 with the increase of iterations, and it is described as follows:

$$a = 2 - 2 \times \frac{t}{t_{\max}} \tag{24}$$

where t_{max} represents the preset maximum number of iterations.

2) Bubble-net attacking strategy

In this phase, two main approaches are designed to imitate the bubble-net attacking strategy, which include shrinking encircling mechanism and spiral updating mechanism. Shrinking encircling mechanism is achieved through the decreasing value of a. The value of auxiliary coefficient vector A is in the interval [-a, a]. Spiral updating mechanism can be modeled as follows:

$$X_p = | X_{best}(t) - X(t) | \times e^{bl} \times \cos(2\pi l) \tag{25}$$

$$X(t+1) = X_p + X_{best}(t) \tag{26}$$

where b is a constant number and l is a random number in the interval [-1, 1].

In the WOA algorithm, the two mentioned approaches of the bubble-net attack strategy can be performed simultaneously. The model can be expressed as follows:

$$X(t+1) = \begin{cases} X_{best}(t) - A \times D, & if \ p < 0.5 \\ X_p + X_{best}(t), & if \ p \ge 0.5 \end{cases} \tag{27}$$

3) Searching randomly strategy

In order to improve the quality of the optimal solution and avoid the local optimal solution, the strategy of searching for the prey randomly is designed. The model can be expressed as follows:

$$D = | C \times X_{rand}(t) - X(t) | \tag{28}$$

$$X(t+1) = X_{rand}(t) - A \times D \tag{29}$$

where X_{rand} is a random individual which is selected from the current candidate solutions.

B. Multi-objective solution strategy

In the MOOPF problem, all the objectives conflict and compete with each other in the power system, and zero-violation of constraints is the premise of ensuring the accuracy of the solutions. Therefore, the quality of candidate solutions should be checked by the Newton-Raphson load flow calculation [23]. In the WOA algorithm, each humpback whales must observe strict rules to the update its position. Based on constrains-prior Pareto-dominant rule, all the candidate whales can be divided into different levels, then the whales in the same level are sorted by the crowding distance and rank value of each whale.

1) CPDR rule

The optimal solution sets are updated with the increase of iterations, each solution should satisfy the ECs and ensure zero-violation. In addition, the handling method of ICs about control variables can be expressed as (30).

$$u_{ith} = \begin{cases} u_{ith\_\max}, & u_{ith} > u_{ith\_\max} \\ u_{ith}, & u_{ith\_\min} < u_{ith} < u_{ith\_\max} \\ u_{ith\_\min}, & u_{ith} < u_{ith\_\min} \end{cases} \tag{30}$$

For the ICs on state variables of each individual whale, the Constrains-prior Pareto-dominant rule (CPDR) is proposed to deal with the problem. The total sum of violations can be expressed as (31).

$$Sv(u_{ith}) = \sum_{j=1}^{Nu} \max(h_j(x, u_{ith}), 0) \tag{31}$$

where Nu is the number of ICs. $Sv(u_{ith})$ represents the total violations of ICs on state variables.

Then, the individuals u_p and u_q are selected from candidate solutions set randomly. Based on the CPDR rule, a smaller $Sv(u)$ value means higher priority, and the kth fitness value is expressed as $f_k(u)$. The process of CPDR rule to find a dominant individual is shown as follows:

Constrains-prior Pareto-dominant Rule:

1. if $Sv(u_p) < Sv(u_q)$ u_p dominates u_q;
2. if $Sv(p_p) > Sv(p_q)$ u_q dominates u_p;
3. if $Sv(p_p) = Sv(p_q)$
4. if $f_i(u_p) \le f_i(u_q)$ for all $i \in \{1, 2, \ldots, M\}$ and $f_j(u_p) < f_j(u_q)$ for any $j \in \{1, 2, \ldots, M\}$
   p_p dominates p_q;
5. else u_q dominates u_p.

According to the CPDR rule, all Candidate solutions set can be divided into m levels: Lev_1, Lev_2, Lev_3…, Lev_m, and *rank* represents the hierarchical level value. The ith individual with the smaller *rank*(i) value means a higher priority.

2) CDRS strategy

All the candidate solutions are divided into different hierarchy by the CPDR strategy. Furthermore, a sorting method based on crowding distance and rank strategy (CDRS) is employed to obtain a high-quality solution [24,25]. According to the CDRS strategy, if the rank values of different whales are equal, their priority statue needs to be determined by the crowding distance. The crowding distance of whale *i* can be defined as *C-dis(i)*, which is used to estimate the density of whales' distribution in the feasible region. With the innovative CDRS strategy, the smaller rank means a better priority. Otherwise, if both solutions obtain the same rank value, then we prefer the solutions with larger *C-dis(i)* value. For any whale *i* and whale *j*, the novel CDRS strategy will be shown as follows:

A Sorting Method With Crowding Distance And Rank Strategy:

1. if $rank(x_i) < rank(x_j)$ whale *i* is stronger than whale *j*.;
2. if $rank(x_i) > rank(x_j)$ whale *j* dominates whale *i*.;
3. if $rank(x_i) = rank(x_j)$
4. if $C\text{-}dis\,(x_i) > C\text{-}dis\,(x_j)$ whale *i* is superior to whale *j*;
5. else whale *j* dominates whale *i*.

3) BCs based on Fuzzy Theory

Taking advantage of the CDRS strategy, the optimal solutions set (POS) obtained by the improved whale optimization algorithm are able to achieve a better quality. The fuzzy theory adopted in this paper can pick out the best compromise solution (BCs) from the POS. The satisfaction degree of *p*th objective for the *k*th whale can be defined as (33), and the total satisfaction degree can be defined as (34).

$$k_p = \begin{cases} 1 & f_p \le f_{p\_\min} \\ \dfrac{f_{p\_\max} - f_i}{f_{p\_\max} - f_{p\_\min}} & f_{p\_\min} < f_p < f_{p\_\max} \\ 0 & f_p \ge f_{p\_\max} \end{cases} \tag{32}$$

$$p = 1, 2, \cdots M_t$$

$$Fst_p = \frac{\sum_{p=1}^{M_t} k_p}{\sum_{j=1}^{N_t} \sum_{p=1}^{M_t} k_p}, \quad j = 1, 2, \cdots N_t \tag{33}$$

where k_p is the standardized satisfaction degree. Fst_p represents the total satisfaction degree.

C. MONIWOA algorithm

1) Piecewise non-linear strategy

In the basic whale optimization algorithm, *A* is coefficient vector to balance the global exploration and local development capabilities. The optimization process is determined by the value of convergence factor *a*. The larger value of *a* indicates stronger global search ability, and the smaller value of *a* indicates stronger local development capabilities inversely. The algorithm is easy to fall into local optimum in the middle and late iterations. Hence, the piecewise non-linear strategy is proposed to prevent falling into the local optimum in the optimization process, and the strategy is described as follows:

$$a(t) = \begin{cases} 2 + \dfrac{-1.8}{1 + e^{-r(2t - t_{max})/2t_{max}}} & t \leqslant 0.75 t_{\max} \\ 3^{\frac{t_{max} - t}{t_{max}}} - 1 & \text{otherwise} \end{cases} \tag{34}$$

where *r* is regulatory factor and the value can be set as 20.

In the piecewise non-linear strategy, the convergence factor *a* can maintain a larger value to increase the global search ability of the WOA algorithm and convergence speed at the beginning. Theoretically, if the iterations reach $0.75t_{max}$, the value of convergence factor *a* can decrease quickly, which helps to realize a rapid transmation into local search. In the end of iteration, a small value is used to ensure the efficiency of local search.

2) Dual dynamic weights mode

The dual dynamic weight mode is able to balance the local and global ability of the whale optimization algorithm. Weight w_1 is used to improve the global search ability, and the weight w_2 is used to improve the local search ability. The mathematical model of special strategy can be expressed as follows:

$$w_1 = (1 - t / t_{\max})^{1 - \tan(pi \times (rand1 - 0.5) \times sm / t_{\max})} \tag{35}$$

$$w_2 = (2 - 2 \times t / t_{\max})^{1 - \tan(pi \times (rand1 - 0.5) \times sm / t_{\max})} \tag{36}$$

where *pi* is a constant number and can be set as π. *sm* is changed with the increasing number of iterations. *sm* will be automatically added if the position of optimal solution is updated, otherwise it will remain unchanged. The update process of *sm* is given as follows:

$$\begin{aligned} & for \quad i = 2 : t_{\max} \\ & \quad if \quad (OP_{cur} > OP_{last}) \\ & \qquad sm = sm + 1 \\ & \quad end \\ & end \end{aligned} \tag{37}$$

where the quality of optimal solution obtained by the calculation of current iterative is defined as OP_{cur}, and the quality of the optimal solution that retained by the previous generation is defined as OP_{last}. In the updating strategy of weight w_1, the mathematical model can be given by the formula as follows:

$$X(t+1) = w_1 \times X_{best}(t) - A \times D \tag{38}$$

$$X(t+1) = X_p + w_1 \times X_{best}(t) \tag{39}$$

$$X(t+1) = w_1 \times X_{rand}(t) - A \times D \tag{40}$$

In the updating strategy of weight w_1, the mathematical model can be expressed as follows:

$$X(t+1) = X_{best}(t) - w_2 \times A \times D \tag{41}$$

$$X(t+1) = w_2 \times X_p + X_{best}(t) \tag{42}$$

$$X(t+1) = X_{rand}(t) - w_2 \times A \times D \tag{43}$$

3) Lévy flight mechanism

With the characteristics of power-law distribution, Lévy flight is a special mechanism which can realize random walk by using Lévy flight distribution [26]. Larger step length can occur by the addition of Lévy flight methodology, and it can escape from local optional solutions and improve the convergence performance [27]. The Lévy flight mechanism can be expressed as follows:

$$\mathrm{Levy}(\lambda) \sim \frac{\mu}{|v|^{1/\beta}}, \quad 0 < \beta < 2 \tag{44}$$

$$\mu \sim \mathrm{N}(0, \sigma_\mu^2), \quad \nu \sim \mathrm{N}(0, \sigma_\nu^2) \tag{45}$$

$$\sigma_\mu = \left\{ \frac{\Gamma(1+\beta) \times \sin(\pi \times \beta / 2)}{\Gamma\left\{\left[(1+\beta)/2\right] \times \beta \times 2^{(\beta-1)/2}\right\}} \right\}^{1/\beta}, \sigma_\nu = 1 \tag{46}$$

where μ and υ are random numbers, which are obtained from the distribution of Gaussian. Γ represents the standard Gamma function. β is a constant number.

$$X(t+1) = X(t) + \alpha \times \frac{\mu}{|v|^{1/\beta}} \times \left(X(t) - X_{best}(t)\right) \times r \quad (47)$$

where r represents a random number in [0, 1]. α is a constant whose value is usually taken as 0.01.

D. Examining the performance of MONIWOA

In order to evaluate the performance of the proposed MONIWOA algorithm, six benchmark test functions are applied to take examination. The comprehensive parameters of the six test functions are set in TABLE I. The convergence curves of the six test functions are displayed in Fig. 1, which demonstrate that the MONIWOA algorithm significantly outperforms the WOA algorithm in convergence accuracy and convergence speed. What's more, the experimental results of those test functions are listed in TABLE II, and the comparison of the experimental results shows that the MONIWOA algorithm is able to obtain better solution than the WOA algorithm in all cases. In summary, the comprehensive performance of the MONIWOA algorithm is better than the WOA algorithm.

E. Application of the MONIWOA to the MOOPF problem

In order to verify the effectiveness of the proposed MONIWOA algorithm, CPDR rule and CDRS strategy, eight test cases were executed in IEEE 30-bus, IEEE 57-bus and IEEE 118-bus systems in Section IV. The POS and BCs obtained by the MONIWOA, MODE and MOPSO algorithms are shown in detail. The main flow chart of MONIWOA algorithm for the MOOPF problem is shown in Fig. 2. The objective combinations of the eight cases are shown in TABLE III.

TABLE I
DESCRIPTION OF THE SIX TEST FUNCTIONS

Name	Functions	Dim	Range of search	f_{min}	Iterations	Running times
Sphere	$f_1(X) = \sum_{i=0}^{D} x_i^2$	30	[–100, 100]	0	1500	30
Rosenbrock	$f_2(X) = \sum_{i=1}^{D-1}\left[100(x_{i+1} - x_i^2)^2 + (x_i - 1)^2\right]$	30	[–30, 30]	0	5000	30
Rastrigin	$f_3(X) = \sum_{i=1}^{D}\left[x_i^2 - 10\cos(2\pi x_i) + 10\right]$	30	[–5.12, 5.12]	0	3000	30
Alpine	$f_4(X) = \sum_{i=1}^{D}\left\|x_i \sin x_i + 0.1x_i\right\|$	30	[–10, 10]	0	1500	30
Goldstein-Price	$f_5(X) = \left[1 + (x_1 + x_2 + 1)^2 \left(19 - 14x_1 + 3x_1^2 - 14x_2 + 6x_1x_2 + 3x_2^2\right)\right] \times \left[(2x_1 - 3x_2)^2 \left(18 - 32x_1 + 12x_1^2 + 48x_2 - 36x_1x_2 + 27x_2^2\right) + 30\right]$	2	[–2, 2]	3	5000	30
Shekel's Family	$f_6(X) = -\sum_{i=1}^{10}\left[(X - a_i)(X - a_i)^T + c_i\right]^{-1}$	4	[0, 10]	-10.5363	8000	30

TABLE II
PERFORMANCE EVALUATION OF THE BENCHMARK TEST FUNCTIONS IN TABLE I

F	WOA				MONWOA			
	Best	Worst	Mean	Deviation	Best	Worst	Mean	Deviation
f_1	2.2012E+01	1.0742E+02	5.4819E+01	2.0265E+01	**8.6873E-47**	**4.7568E-44**	**6.1928E-45**	**1.0994E-44**
f_2	3.6414E+01	1.4721E+02	7.0394E+01	1.4964E+01	**9.7863E-10**	**7.8662E-06**	**4.1287E-07**	**1.6862E-06**
f_3	9.8334E+01	2.2785E+02	1.5557E+02	2.8023E+01	**1.6914E+01**	**6.8652E+01**	**3.7875E+01**	**1.2743E+01**
f_4	1.4446E+01	2.3956E+01	1.9057E+01	2.2052E+00	**6.6613E-16**	**1.0936E-14**	**3.2474E-15**	**2.7989E-15**
f_5	3.0000E+00	3.0141E+00	3.0012E+00	9.1472E-05	**3.0000E+00**	**3.0000E+00**	**3.0000E+00**	**1.0408E-16**
f_6	-1.0526E+01	-1.0482E+01	-1.0510E+01	7.8628E-03	**-1.0536E+01**	**-1.0536E+01**	**-1.0536E+01**	**1.8373E-12**

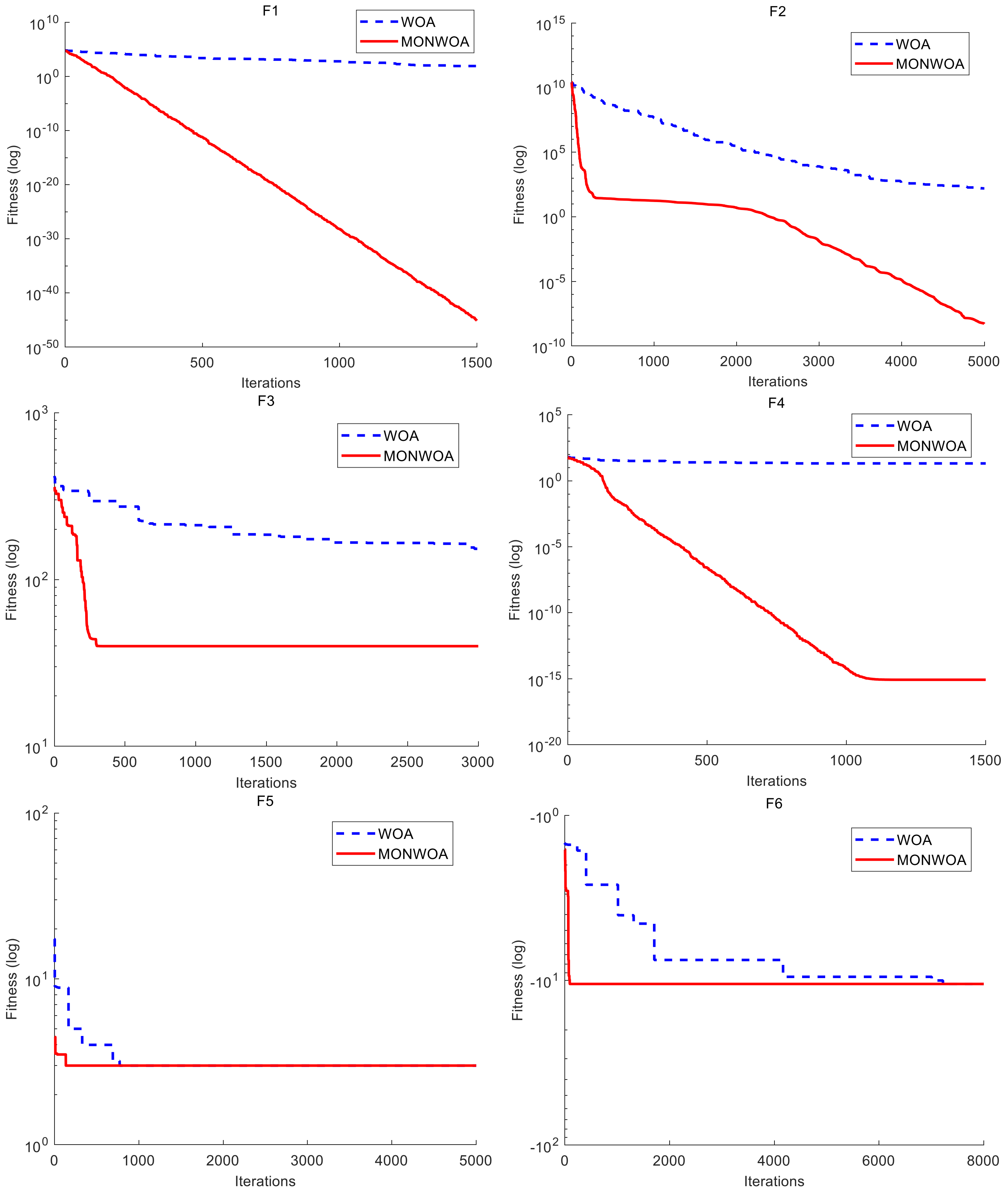

Fig. 1. Convergence graphs of WOA and MONIWOA for six representative test functions

TABLE III
THE OBJECTIVE COMBINATION OF THE THREE ALGORITHMS

The objective combination	*Fc*	P_l	*F-v*	E_m	*L-in*	Test system
CASE 1	✔			✔		IEEE 30
CASE 2		✔			✔	IEEE 30
CASE 3		✔	✔			IEEE 30
CASE 4	✔	✔		✔		IEEE 30
CASE 5	✔	✔				IEEE 57
CASE 6	✔			✔		IEEE 57
CASE 7	✔	✔				IEEE 118
CASE 8	✔			✔		IEEE 118

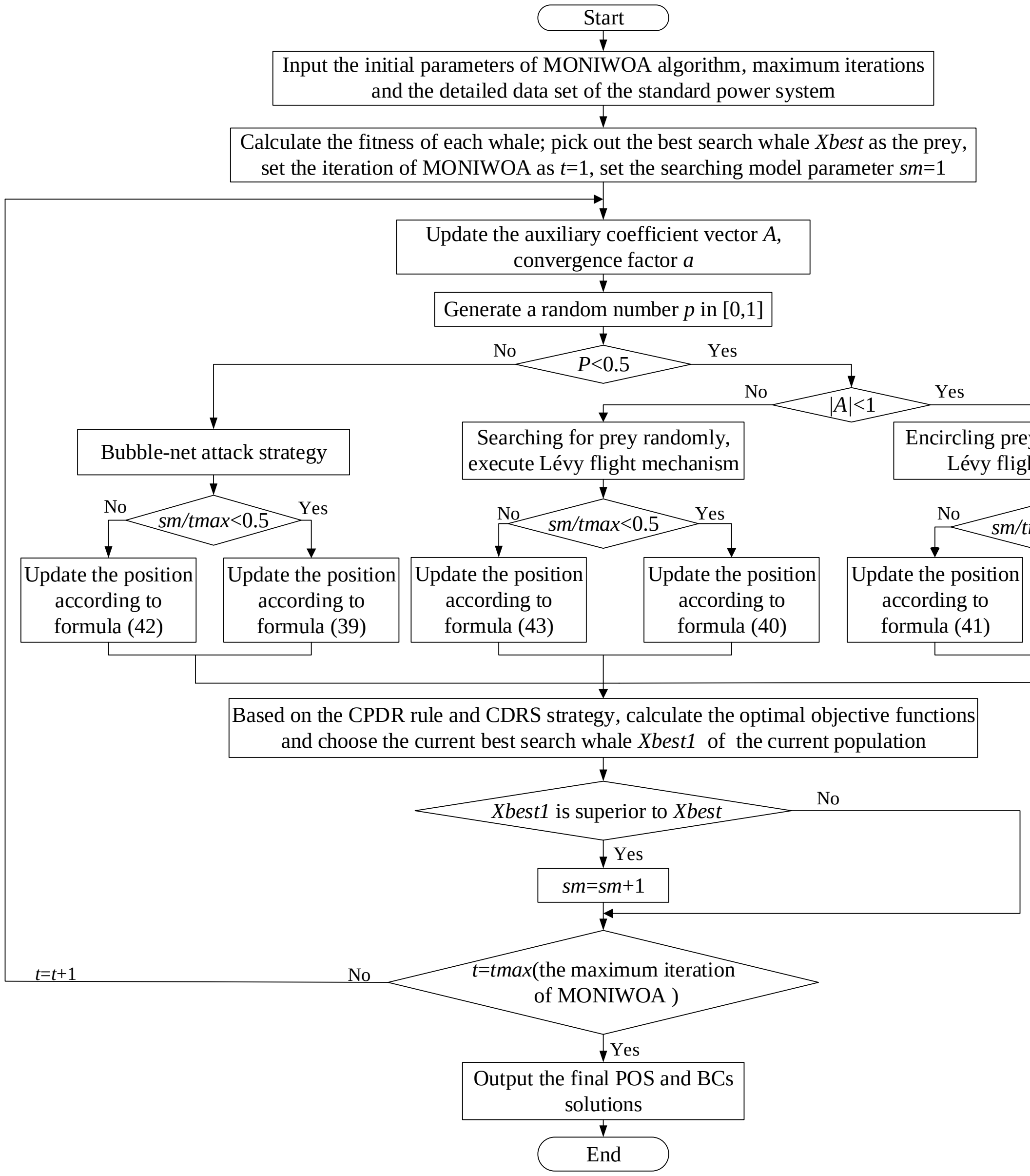

Fig. 2. The flow chart of MONIWOA for the MOOPF problem

IV. SIMULATION AND RESULT

To substantiate the performance of WONIWOA algorithm, MOPSO and MODE algorithms are employeed as comparisons, and the three algorithms are all applied to solve the MOOPF problem in the simulation trials. Eight simulation trials which include seven bi-objectives and one tri-objectives have been tested in IEEE 30-bus system (system1), IEEE 57-bus system (system2) and IEEE 118-bus system(system3). All the experimental programs are coded in the MATLAB 2017b and run on a Microsoft Windows 7 PC with Intel(R) Core (TM) i5-7400 CPU @ 3.4GHZ with 8GB RAM.

A. Parameters setting

1) System parameters

The wiring diagram of the IEEE 30-bus system includes 24-dimensional control variables and is shown in Fig. 3. In system1, the value of transformer taps are set in [0.9 1.1] p.u and the value of voltage of generator buses and load buses are set in [0.95 1.1] p.u. The detail data of system1 are given in [28], and the coefficients of *Fcost* and *Em* in IEEE 30-bus system can been seen in [29].

The wiring diagram of the IEEE 57-bus system is shown in Fig. 4, and it has 33-dimensional control variables. In system2, the value of transformer taps are set in [0.9 1.1] p.u, and the value of voltage magnitude for *PQ* and *PV* bus are set in [0.95 1.1] p.u. The detail data of system2 are given in [30].

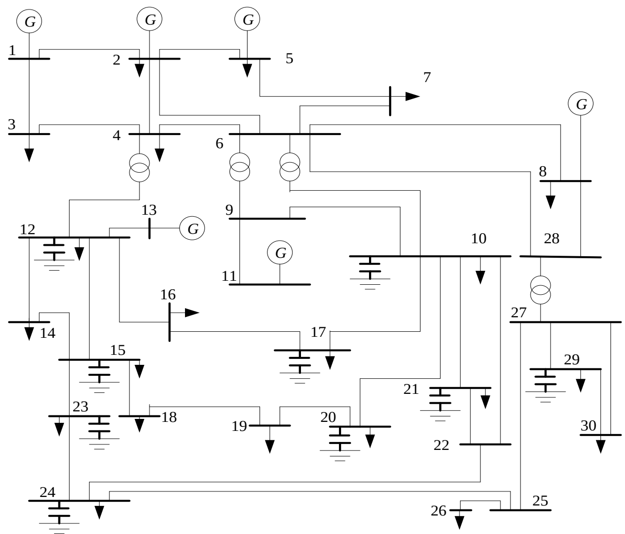

Fig. 3. The wiring diagram of the IEEE 30-bus system

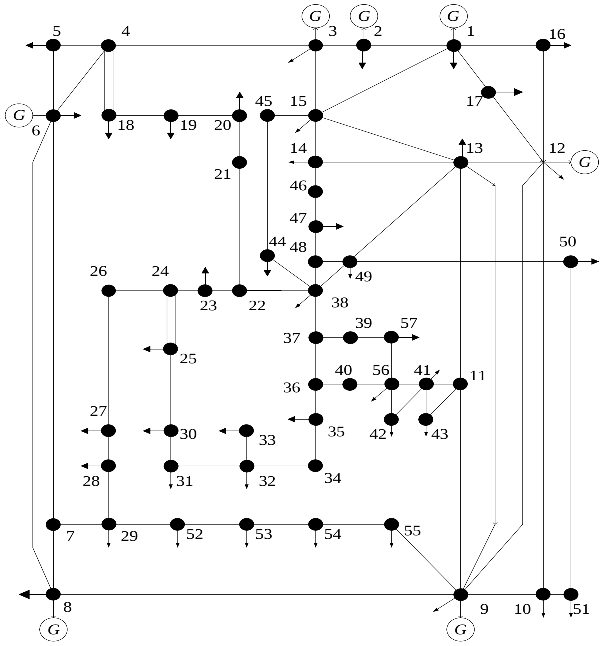

Fig. 4. The wiring diagram of the IEEE 57-bus system

The structure of the IEEE 118-bus system includes 128-dimensional control variables and is shown in Fig. 5. The value of voltage magnitude for PV bus are set in [0.95 1.1] p.u. The detail data of system3 are given in [30].

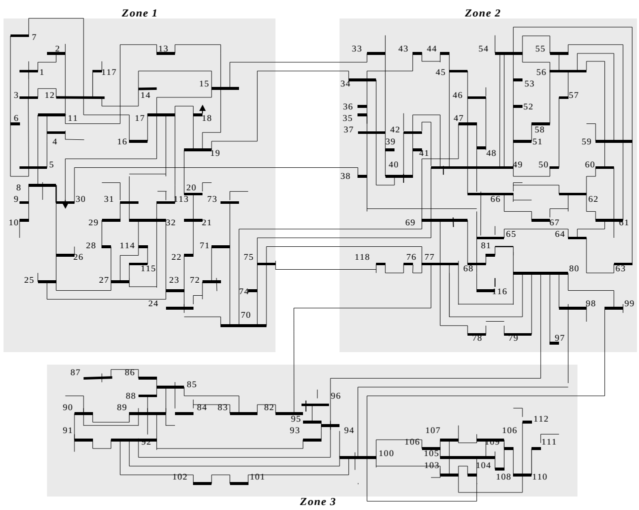

Fig. 5. The wiring diagram of the IEEE 118-bus system

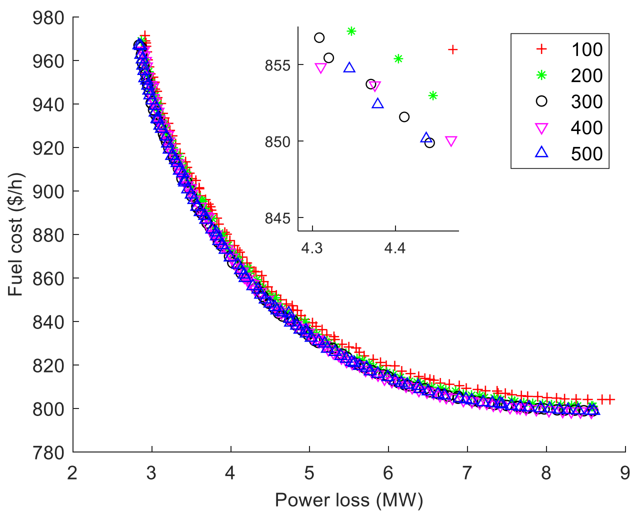

Fig. 6. PFs with different iterations of the IEEE 30-bus system

2) Algorithm parameters

The effectiveness and accuracy of the MONIWOA algorithm are mainly determined by the maxinum iterations and population size. Then repeated simulation experiments of the three standard test systems are carried out in different iterations. As is shown in Fig. 6- Fig. 7, the PFs obtained in 400 iterations and 500 iterations have no obvious superority over PFs obtained in 300 iterations in the IEEE 30-bus and IEEE 57-bus systems. As is shown in Fig. 8, the PFs obtained in 500 iterations are relatively better in the IEEE 118-bus systems. Therefore, the maxinum iterations are set as 300 in the IEEE 30-bus and IEEE 57-bus systems, the maxinum iterations are set as 500 in the IEEE 118-bus system. The population size is set as 100. The parameters of the three algorithms are shown in TABLE IV. After a set of repeated trials, the MONIWOA algorithm can pick up the uniform PFs finally.

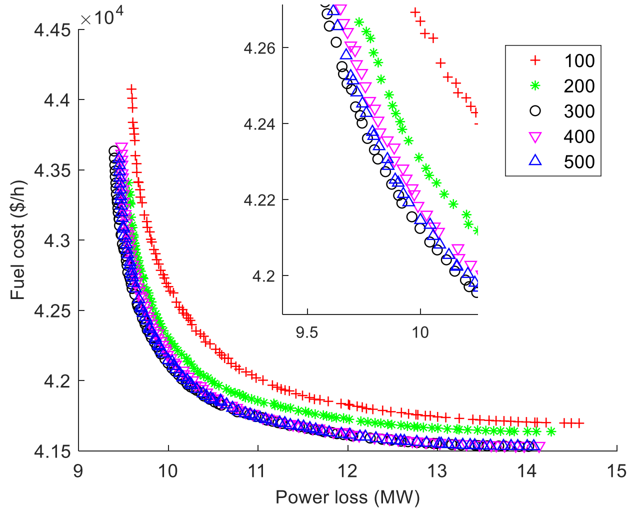

Fig. 7. PFs with different iterations of the IEEE 57-bus system

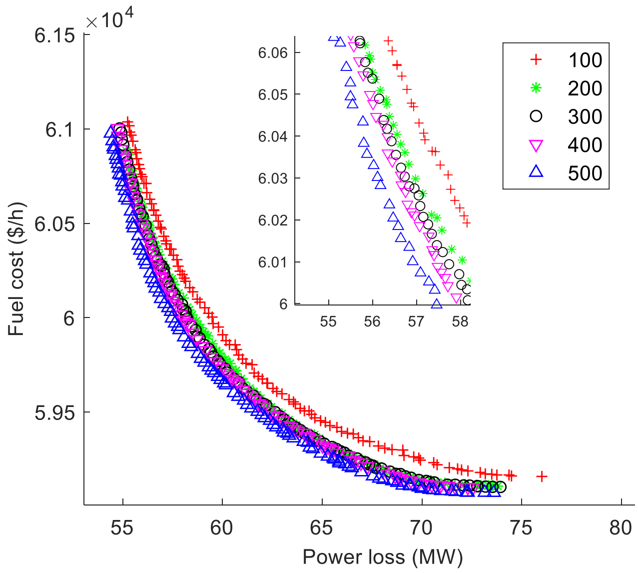

Fig. 8. PFs with different iterations of the IEEE 118-bus system

B. Trials on IEEE 30-bus system

1) CASE 1: Optimizing *Fc* and *Em* simultaneously

In CASE 1, *Fc* and *Em* are optimized by the MONIWOA, MODE and MOPSO algorithms in the system1 simultaneously. Fig. 9 shows the distribution of PFs obtained by the MONIWOA, MODE and MOPSO algorithms, and it can be found intuitively that MONIWOA's POS is more widely distributed and has better distribution uniformity. Two boundary solutions (the minimum *Fc* and minimum *Em*) and the BCs are given in Fig. 10 by using the MONIWOA approach. The detailed data of control variables of the BCs obtained by the MONIWOA algorithm can be seen in TABLE V, and it is clearly seen that 834.1110 \$/h of *Fc* and 0.2311 ton/h of *Em*. The bi-objective function values and PFs obtained in CASE 1 clearly demonstrates that the proposed novel approach dominates the BCs of MOPSO and MODE algorithms. Additionally, in order to prove the superiority of the MONIWOA, comparison results of BCs obtained by other reported algorithms are shown in TABLE VI.

TABLE IV
THE PARAMETERS OF THE THREE ALGORITHMS

Algorithms	Parameters	Values
General parameters	Population	100
	Repository	100
	t_{max}	300(CASE 1-CASE 6) 500(CASE 7-CASE 8)
MONIWOA	σ	1
	μ	0
	b	1
	RR	0.6
	sm	1
MODE	b	1
MOPSO	C_1	2
	C_2	2
	ω	0.85

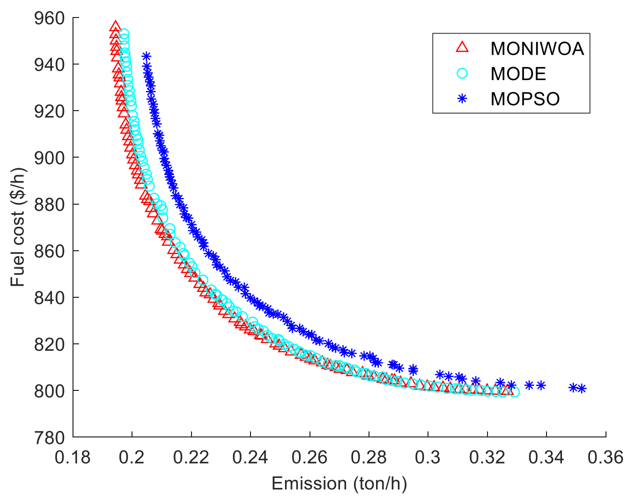

Fig. 9. The PFs of MONIWOA, MODE and MOPSO for CASE 1

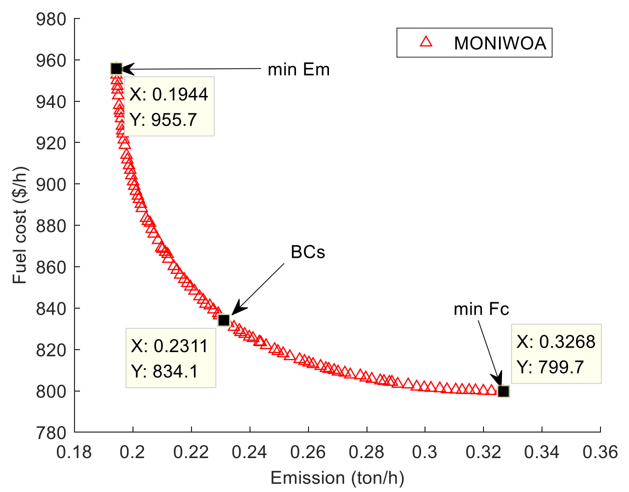

Fig. 10. The PFs of MONIWOA in CASE 1

2) CASE 2: Optimizing *L_in* and P_l simultaneously

L_in is an important indicator to measure voltage stability in the actual power system. The smaller value of *L_in* means the stronger stability and better operating status of the power system.

In CASE 2, *L_in* and P_l are optimized by the MONIWOA, MODE and MOPSO algorithms in the system1 simultaneously. Fig. 11 gives the optimal PFs obtained by different algorithms, and the comparisons of PFs among the three algorithms clearly demonstrate that POS of MONIWOA is more widely distributed and has better distribution uniformity. Two boundary solutions (the minimum *L_in* and minimum P_l) and the BCs obtained by the MONIWOA approach are given in Fig. 12. The detail data of control variables and BCs are shown in TABLE VII. The BCs of MONIWOA are 0.1244p.u. of *L_in* and 2.8620 MW of P_l, and they are smaller than those obtained by MODE and MOPSO respectively. Therefore, the results show that the performance of MONIWOA algorithm is better than MODE and MOPSO algorithms when dealing with the MOOPF problem.

TABLE V
CONTROL VARIABLES OF BCS FOR CASE 1

control variables	MOPSO	MODE	MONIWOA
P_2(MW)	59.7749	58.9058	61.4488
P_5(MW)	26.8345	27.3974	27.2159
P_8(MW)	34.7677	34.7373	35.0000
P_{11}(MW)	29.0368	27.3819	27.0870
P_{13}(MW)	25.1815	25.8972	24.3510
V_1(p.u)	1.1000	1.0990	1.1000
V_2(p.u)	1.0827	1.089	1.0831
V_5(p.u)	1.0561	1.0560	1.0566
V_8(p.u)	1.0870	1.0795	1.0772
V_{11}(p.u)	1.0708	1.0936	1.0471
V_{13}(p.u)	1.0865	1.0760	1.0796
T_{11}(p.u)	1.0671	1.0651	1.0181
T_{12}(p.u)	0.9440	0.9448	0.9832
T_{15}(p.u)	0.9419	1.0103	1.0407
T_{36}(p.u)	1.0314	0.9767	0.9893
Q_{10}(p.u)	0.0500	0.0098	0.0431
Q_{12}(p.u)	0.0000	0.0419	0.0277
Q_{15}(p.u)	0.0378	0.0407	0.0224
Q_{17}(p.u)	0.0326	0.0283	0.0265
Q_{20}(p.u)	0.0222	0.0111	0.0205
Q_{21}(p.u)	0.0212	0.0238	0.0496
Q_{23}(p.u)	0.0500	0.0235	0.0257
Q_{24}(p.u)	0.0235	0.05	0.0331
Q_{29}(p.u)	0.0003	0.0249	0.0359
Obj1 (\$/h)	836.2408	834.9988	**834.1110**
Obj2(ton/h)	0.2489	0.2431	**0.2311**

TABLE VI
COMPARISON RESULTS FOR CASE 1

Algorithm	*Fc* (\$/h)	*Em* (ton/h)
NSGA-II [1]	837.7028	0.2434
NSGA-III [23]	836.4405	0.2423
PSO [32]	883.2800	0.2388
GSO [32]	852.8900	0.2446
ASGO [33]	843.5473	0.2539

3) CASE 3: Optimizing *F_v* and P_l simultaneously

In CASE 3, due to the typical non-convexity of value-point effect, it is more difficult to optimize *F_v* and P_l simultaneously to solve the MOOPF problem. The optimal PFs obtained by different algorithms are shown in Fig. 13, it is evidently proved that the MONIWOA approach has the ability to pick up the more appropriate PFs as compared to MODE and MOPSO algorithms. Two boundary solutions (the minimum *F_v* and minimum P_l)and the BCs are given in Fig. 14 by using the MONIWOA approach. The detail results are shown in TABLE VIII. It is clearly seen that 858.7143 \$/h of F_v and 5.9125 MW of P_l for the MONIWOA's BCs, which is narrowly smaller than the BCs of MODE and MOPSO concurrently. In summary, the results prove that MONIWOA approach can seek out the better quality of BCs.

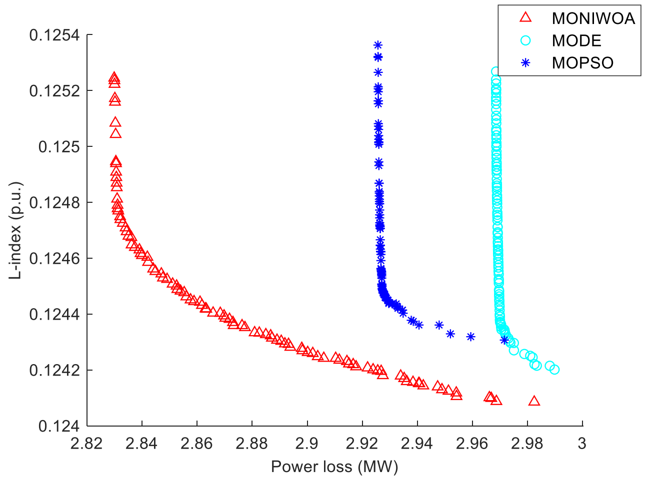

Fig. 11. The PFs of MONIWOA, MODE and MOPSO for CASE 2

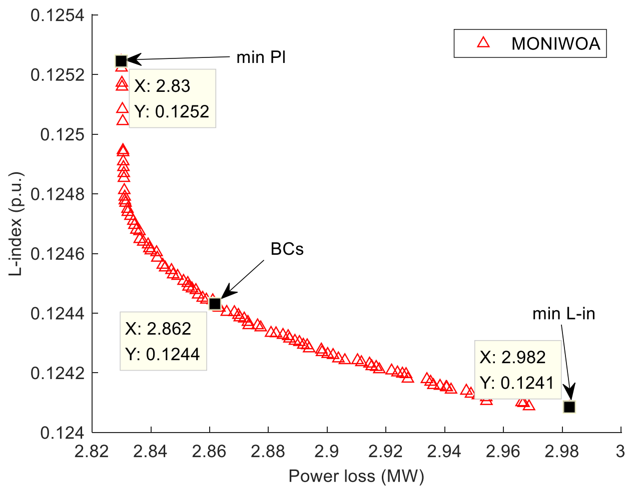

Fig. 12. The PFs of MONIWOA in CASE 2

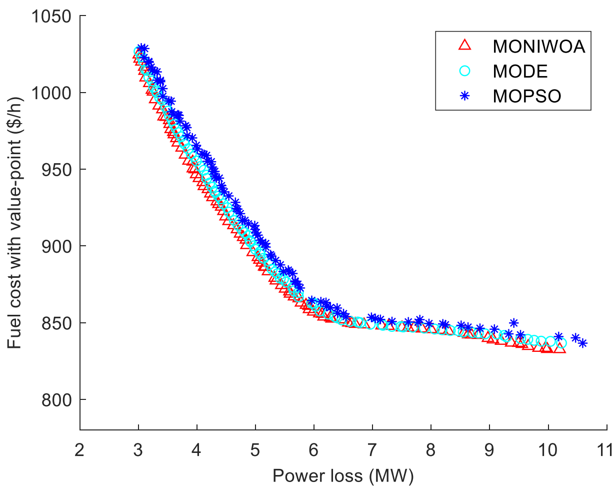

Fig. 13. The PFs of MONIWOA, MODE and MOPSO for CASE 3

4) CASE 4: Optimizing *Fc*, P_l and *Em* simultaneously

In CASE 4, a tri-objective optimization simulation which includes objective functions of *Fc*, P_l *and Em* are tested in system1 simultaneously, so it is difficult to obtain the appropriate PFs and BCs. The optimal PFs of the MONIWOA, MODE and MOPSO algorithms are shown in Fig. 15, it is obviously demonstrated that the quality of PFs obtained by MONIWOA method is better than others. The BCs of MONIWOA method is given in Fig. 16.

TABLE VII

CONTROL VARIABLES OF BCS FOR CASE 2

control variables	MOPSO	MODE	MONIWOA
P_2(MW)	79.8749	79.9903	79.9821
P_5(MW)	50.0000	49.9951	49.9927
P_8(MW)	35.0000	35.0001	35.0000
P_{11}(MW)	30.0000	29.9879	29.9938
P_{13}(MW)	40.0000	39.9998	39.9954
V_1(p.u)	1.1000	1.0907	1.1000
V_2(p.u)	1.1000	1.1000	1.0992
V_5(p.u)	1.1000	1.0952	1.0848
V_8(p.u)	1.0900	1.1000	1.0930
V_{11}(p.u)	1.1000	1.0987	1.0998
V_{13}(p.u)	1.1000	1.0941	1.0998
T_{11}(p.u)	1.0673	1.0722	1.0434
T_{12}(p.u)	0.9000	0.9000	0.9001
T_{15}(p.u)	0.9963	0.9852	0.9946
T_{36}(p.u)	0.9770	0.9718	0.9641
Q_{10}(p.u)	0.0500	0.0500	0.0392
Q_{12}(p.u)	0.0500	0.0000	0.0473
Q_{15}(p.u)	0.0356	0.0482	0.0498
Q_{17}(p.u)	0.0500	0.0500	0.0500
Q_{20}(p.u)	0.0331	0.0500	0.0400
Q_{21}(p.u)	0.0500	0.0490	0.0500
Q_{23}(p.u)	0.0245	0.0419	0.0190
Q_{24}(p.u)	0.0500	0.0200	0.0424
Q_{29}(p.u)	0.0203	0.0182	0.0047
Obj1 (MW)	2.9284	2.9278	**2.8620**
Obj2(p.u.)	0.1245	0.1247	**0.1244**

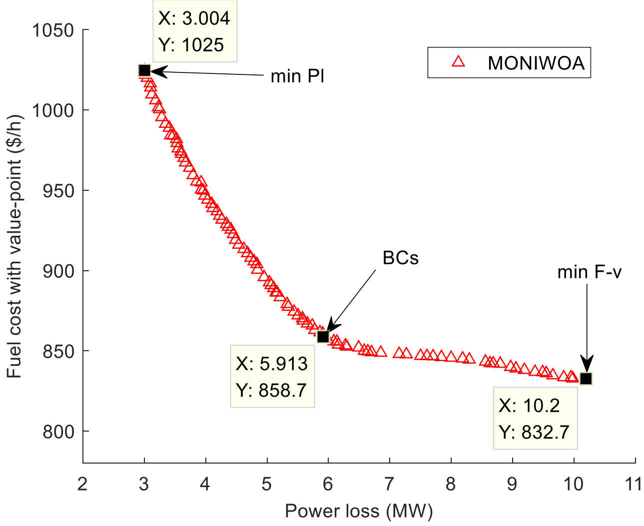

Fig. 14. The PFs of MONIWOA in CASE 3

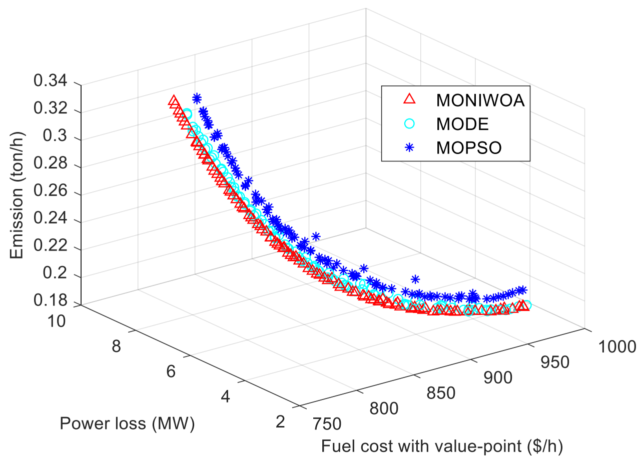

Fig. 15. The PFs of MONIWOA, MODE and MOPSO for CASE 4

Additionally, the detail results of CASE 4 are shown in TABLE IX, it is intuitively found that *Fc*, P_l and *Em* are 869.6487 $/h, 4.0972 MW and 0.2099 ton/h correspondingly by using the proposed method. The BCs solution of MODE algorithm includes 879.8652 $/h of *Fc*, 4.1630 MW of P_l and 0.2129 ton/h of *Em*. The BCs solutions of MOPSO algorithm includes 881.6949 $/h of *Fc*, 4.1408 MW of P_l and 0.2161 ton/h of *Em*. The detail results clearly show that the MONIWOA algorithm can pick up the minimum *Fc*, P_l and *Em* at the same time, and it proves that the MONIWOA method has competitive advantages to seek out better optimal solution as compared to other algorithms.

TABLE VIII
CONTROL VARIABLES OF BCS FOR CASE 3

control variables	MOPSO	MODE	MONIWOA
P_2(MW)	53.5011	46.5733	54.0425
P_5(MW)	31.5425	30.9953	30.2594
P_8(MW)	35.0000	34.0947	35.0000
P_{11}(MW)	24.2590	23.5005	21.0240
P_{13}(MW)	12.0000	18.2117	14.5985
V_1(p.u)	1.1000	1.0997	1.1000
V_2(p.u)	1.0852	1.0900	1.0911
V_5(p.u)	1.0626	1.0712	1.0614
V_8(p.u)	1.0656	1.0835	1.0766
V_{11}(p.u)	1.1000	1.0927	1.0973
V_{13}(p.u)	1.0771	1.0902	1.0965
T_{11}(p.u)	1.0016	0.9482	0.9654
T_{12}(p.u)	0.9313	1.0274	0.9900
T_{15}(p.u)	1.0143	0.9898	0.9855
T_{36}(p.u)	0.9677	0.9743	0.9569
Q_{10}(p.u)	0.0445	0.0223	0.0052
Q_{12}(p.u)	0.0219	0.0396	0.0399
Q_{15}(p.u)	0.0351	0.0429	0.0378
Q_{17}(p.u)	0.0363	0.0380	0.0406
Q_{20}(p.u)	0.0500	0.0490	0.0341
Q_{21}(p.u)	0.0500	0.0348	0.0500
Q_{23}(p.u)	0.0267	0.0178	0.0092
Q_{24}(p.u)	0.0310	0.0489	0.0234
Q_{29}(p.u)	0.0067	0.0218	0.0013
Obj1 ($/h)	863.6488	862.6993	**858.7143**
Obj2(MW)	6.1162	5.9186	**5.9125**

TABLE IX
CONTROL VARIABLES OF BCS FOR CASE 4

control variables	MOPSO	MODE	MONIWOA
P_2(MW)	64.2681	64.2492	63.9709
P_5(MW)	40.3384	39.0327	36.8832
P_8(MW)	34.9543	34.9183	34.8272
P_{11}(MW)	29.8791	29.4127	29.0692
P_{13}(MW)	39.6487	33.5994	31.2443
V_1(p.u)	1.1000	1.0989	1.0977
V_2(p.u)	1.0965	1.0913	1.0936
V_5(p.u)	1.0891	1.0713	1.0713
V_8(p.u)	1.0932	1.0833	1.0779
V_{11}(p.u)	1.1000	1.0900	1.0970
V_{13}(p.u)	1.1000	1.0959	1.0977
T_{11}(p.u)	1.0991	1.0129	1.0329
T_{12}(p.u)	0.9000	0.9289	0.9191
T_{15}(p.u)	0.9689	1.0042	1.0188
T_{36}(p.u)	0.9600	0.9966	0.9652
Q_{10}(p.u)	0.0500	0.0300	0.0472
Q_{12}(p.u)	0.0000	0.0500	0.0497
Q_{15}(p.u)	0.0461	0.0041	0.0493
Q_{17}(p.u)	0.0500	0.0431	0.0154
Q_{20}(p.u)	0.0023	0.0216	0.0282
Q_{21}(p.u)	0.0031	0.0500	0.0240
Q_{23}(p.u)	0.0425	0.0174	0.0016
Q_{24}(p.u)	0.0500	0.0047	0.0499
Q_{29}(p.u)	0.0001	0.0451	0.0208
Obj1 ($/h)	881.6949	879.8652	**869.6487**
Obj2(MW)	4.1408	4.1630	**4.0972**
Obj3(ton/h)	0.2161	0.2129	**0.2099**

C. *Trials on IEEE 57-bus system*

1) CASE 5: Optimizing P_l and *Fc* simultaneously

The system2 has 33-dimensional control variables, seventeen transformers and seven generators. Due to the structure of system2 is more complicated when compared with system1, it is more difficult to solve the MOOPF problem in system2.

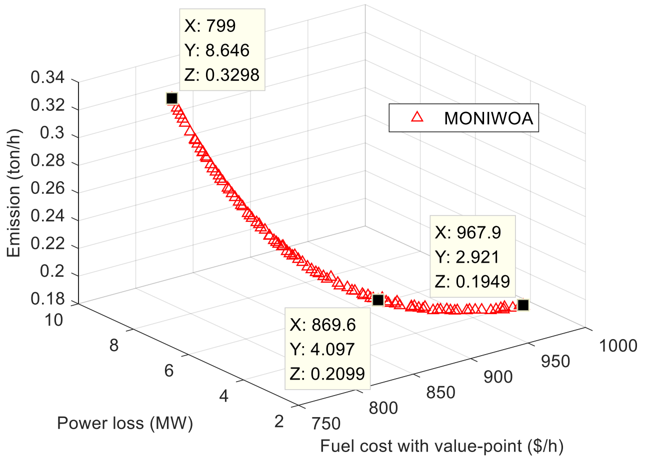

Fig. 16. The PFs of MONIWOA in CASE 4

TABLE X
CONTROL VARIABLES OF BCS FOR CASE 5

control variables	MOPSO	MODE	MONIWOA
P_2(MW)	88.76678	54.4425	72.4938
P_3(MW)	54.2749	60.4878	56.0316
P_6(MW)	90.4244	74.2930	79.6583
P_8(MW)	379.2661	400.8032	385.8774
P_9(MW)	99.3766	99.8446	100.0000
P_{12}(MW)	409.5642	410.0000	410.0000
V_1(p.u.)	1.1000	1.0992	1.1000
V_2(p.u.)	1.1000	1.0954	1.0977
V_3(p.u.)	1.1000	1.0911	1.0940
V_6(p.u.)	1.1000	1.0965	1.0938
V_8(p.u.)	1.1000	1.0992	1.0993
V_9(p.u.)	1.1000	1.0876	1.0999
V_{12}(p.u.)	1.1000	1.0817	1.0950
T_{19}(p.u.)	0.9919	1.0570	1.0878
T_{20}(p.u.)	1.1000	0.9806	1.0754
T_{31}(p.u.)	0.9848	0.9741	1.0276
T_{35}(p.u.)	1.0753	1.0983	0.9851
T_{36}(p.u.)	1.0240	0.9921	1.0794
T_{37}(p.u.)	0.9555	1.0641	1.0762
T_{41}(p.u.)	1.0090	1.0337	1.0220
T_{46}(p.u.)	0.9842	0.9684	0.9246
T_{54}(p.u.)	0.938	0.9707	0.9973
T_{58}(p.u.)	1.1000	0.9805	0.9825
T_{59}(p.u.)	1.1000	0.9580	0.9744
T_{65}(p.u.)	1.1000	0.9747	1.0000
T_{66}(p.u.)	1.0138	0.9416	0.9637
T_{71}(p.u.)	0.9814	0.9845	0.9848
T_{73}(p.u.)	1.0441	0.9431	1.0417
T_{76}(p.u.)	0.9000	1.0493	0.9987
T_{80}(p.u.)	1.0093	1.0135	1.0417
Q_{18}(p.u.)	0.0740	0.167	0.2494
Q_{25}(p.u.)	0.2788	0.1508	0.1931
Q_{53}(p.u.)	0.1307	0.1748	0.2425
Obj1 ($/h)	41970.3869	41964.2468	**41934.6701**
Obj2(MW)	11.8702	11.1124	**10.8410**

In CASE 5, a bi-objective optimization simulation which includes *Fc* and P_l are tested in system2 simultaneously. Fig. 17 shows the comparative curves of optimal PFs obtained by the MONIWOA, MODE and MOPSO algorithms, it is obviously shown that PFs of MONIWOA approach is more superior as compared to MODE and MOPSO algorithms. The boundary solutions and the BCs are shown in Fig. 18. The detail results of CASE 5 are shown in TABLE X. The MONIWOA algorithm can seek out the BCs which includes 41934.6701 $/h of *Fc* and 10.8410 MW of P_l. The BCs of

MODE algorithm includes 41964.2468 \$/h of *Fc* and 11.1124 MW of P_l. The BCs of MOPSO algorithm includes 41970.3869 \$/h of *Fc* and 11.8702 MW of P_l. Therefore, it proves that the MONIWOA approach owns better ability to pick up the BCs.

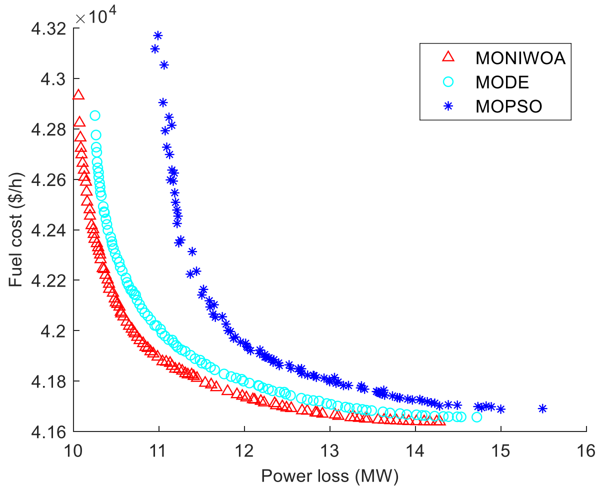

Fig. 17. The PFs of MONIWOA, MODE and MOPSO for CASE 5

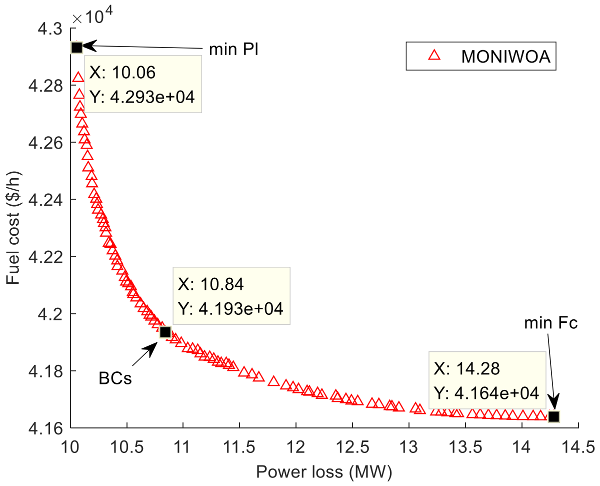

Fig. 18. The PFs of MONIWOA in CASE 5

2) CASE 6: Optimizing *Fc* and *Em* simultaneously

In CASE 6, a bi-objective optimization simulation which includes *Fc* and *Em* are tested in system2 simultaneously. The optimal PFs of the MONIWOA, MODE and MOPSO algorithms are shown in Fig. 19. It is clearly shown that PFs of MONIWOA approach owns better performance, and MONIWOA has the superior ability to seek out high-caliber PFs as compared to others. The boundary solutions and the BCs are shown in Fig. 20.

Detail results of CASE 6 are shown in TABLE XI. The BCs of the MONIWOA approach which includes 43265.8262 \$/h of *Fc* and 1.2096 ton/h of *Em* are smaller than the ones of MODE and MOPSO algorithms respectively, and it is worth paying attention to the superior performance of MONIWOA approach to find the minimum *Fc*. Therefore, the BCs of the MONIWOA approach can completely dominate the ones of other methods.

D. Trials on IEEE 118-bus system

1) CASE 7: Optimizing *Fc* and P_l simultaneously

The structure of system3 is more complicated than system2. In order to verify the effectiveness of MONIWOA to seek out better PFs in system3, then a bi-objective optimization simulation which includes *Fc* and P_l are carried on in system3. It should be noted that the MOPSO algorithm cannot seek out a set of well distributed solutions, so no effective PFs is obtained. The optimal PFs obtained by MONIWOA and MODE methods are illustrated in Fig. 21. It is intuitively shown that the evenly-distribute PFs of MONIWOA algorithm is better. As well, MODE algorithm has a competitive advantage over obtaining densely-distribute PFs. The boundary solutions and the BCs are shown in Fig. 22. BCs obtained by the MONIWOA and MODE methods are shown in TABLE XIII, the BCs of the MONIWOA algorithm includes 58586.8759 \$/h of *Fc* and 56.1994 MW of P_l. The BCs of the MODE algorithm includes 59433.2483 \$/h of *Fc* and 58.1511 MW of P_l. In general, the MONIWOA algorithm owns evident ability to obtain better PFs and smaller BCs as compared to MODE algorithm. Additionally, in order to prove the superiority of the MONIWOA algorithm, comparison results of BCs obtained by other reported algorithms are shown in TABLE XII.

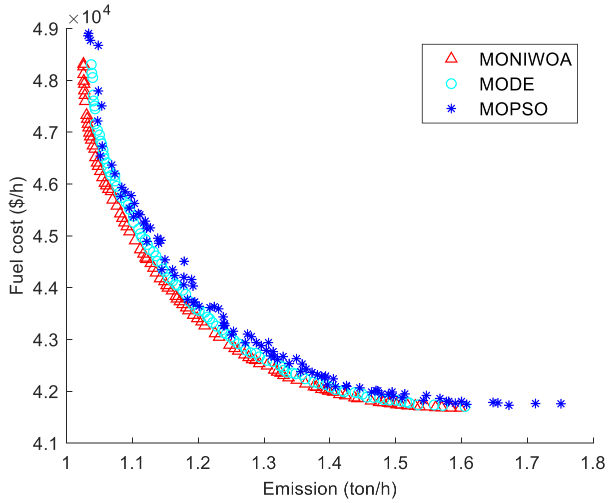

Fig. 19. The PFs of MONIWOA, MODE and MOPSO for CASE 6

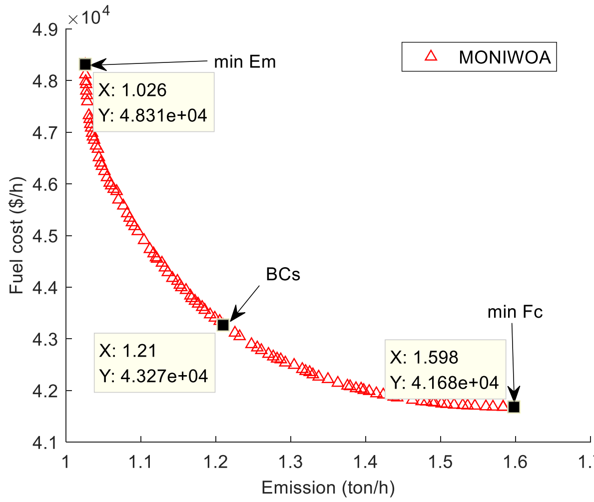

Fig. 20. The PFs of MONIWOA for CASE 6

2) CASE 8: Optimizing *Fc* and *Em* simultaneously

In CASE 8, a bi-objective optimization simulation which includes *Fc* and *Em* are tested in system3. Due to the more complicated structure of system3, no effective PFs is obtained by the MOPSO algorithm. The optimal PFs obtained by MONIWOA and MODE methods are shown in Fig. 23. It is obviously demonstrated that the quality of PFs obtained by MONIWOA method is better. The boundary solutions and the BCs are given in Fig. 24.

TABLE XI

CONTROL VARIABLES OF BCS FOR CASE 6

control variables	MOPSO	MODE	MONIWOA
P_2(MW)	100.0000	99.5394	99.9534
P_3(MW)	84.0305	96.9918	95.6767
P_6(MW)	97.7124	99.2096	99.9345
P_8(MW)	337.6508	355.2533	354.0411
P_9(MW)	100.0000	100.0000	99.9022
P_{12}(MW)	323.7972	280.6742	295.9330
V_1(p.u)	1.1000	1.0998	1.0992
V_2(p.u)	1.1000	1.0988	1.0985
V_3(p.u)	1.0999	1.0954	1.0964
V_6(p.u)	1.1000	1.0992	1.0994
V_8(p.u)	1.1000	1.0983	1.0983
V_9(p.u)	1.1000	1.0984	1.0988
V_{12}(p.u)	1.1000	1.0884	1.0857
T_{19}(p.u)	1.0669	0.9711	1.0795
T_{20}(p.u)	1.0168	1.0192	1.0208
T_{31}(p.u)	1.0123	1.0300	0.9811
T_{35}(p.u)	1.0721	1.0271	0.9934
T_{36}(p.u)	1.0963	1.0014	1.0251
T_{37}(p.u)	1.0311	1.0832	0.9811
T_{41}(p.u)	1.1000	1.0419	1.0247
T_{46}(p.u)	0.9116	1.0202	0.9997
T_{54}(p.u)	0.9341	0.9129	1.0721
T_{58}(p.u)	1.1000	1.0010	1.0060
T_{59}(p.u)	1.0574	1.0191	1.0093
T_{65}(p.u)	1.0784	0.9979	1.0346
T_{66}(p.u)	0.9748	0.9561	0.9815
T_{71}(p.u)	1.0174	1.0214	0.9703
T_{73}(p.u)	1.0170	1.0236	0.9502
T_{76}(p.u)	0.9000	0.9145	1.0048
T_{80}(p.u)	1.0264	1.0839	1.0201
Q_{18}(p.u)	0.0591	0.1247	0.2470
Q_{25}(p.u)	0.2527	0.0986	0.1761
Q_{53}(p.u)	0.0705	0.1598	0.1185
Obj1 ($/h)	43303.9195	43332.2408	**43265.8262**
Obj2(ton/h)	1.2748	1.2141	**1.2096**

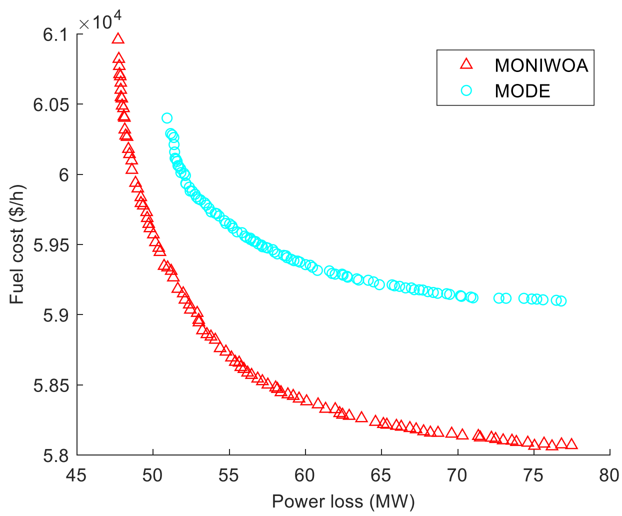

Fig. 21. The PFs of MONIWOA and MODE for CASE 7

BCs obtained by the by MONIWOA and MODE methods are shown in TABLE XIV, the BCs of the MONIWOA algorithm includes 60567.8210 $/h of Fc and 2.5066 ton/h of Em. The BCs of the MODE algorithm includes 60928.7800 $/h of Fc and 2.5886 ton/h of Em. Therefore, it proves that the MONIWOA algorithm owns superior ability to obtain better PFs and smaller BCs as compared to MODE algorithm.

E. Comprehensive evaluation

In order to evaluate the algorithm's efficiency, the average running time in each iteration is utilized to represent the computation complexity. The average running time of the

TABLE XII

COMPARISON RESULTS FOR CASE 7

Algorithm	*Fc* ($/h)	P_l (MW)
NSGA-II [30]	59900.3741	58.8192
NSGA-III [20]	59474.4030	58.4603
HFBA-COFS [30]	59624.0613	61.0362
MOPSO [20]	59133.1054	57.0368

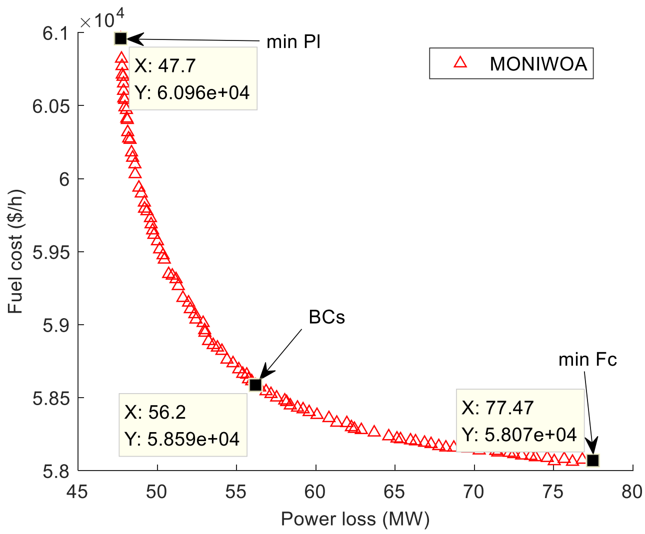

Fig. 22. The PFs of MONIWOA in CASE 7

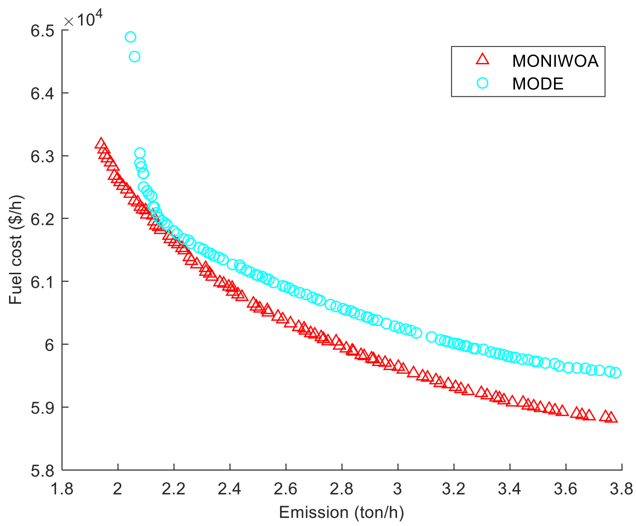

Fig. 23. The PFs of MONIWOA and MODE for CASE 8

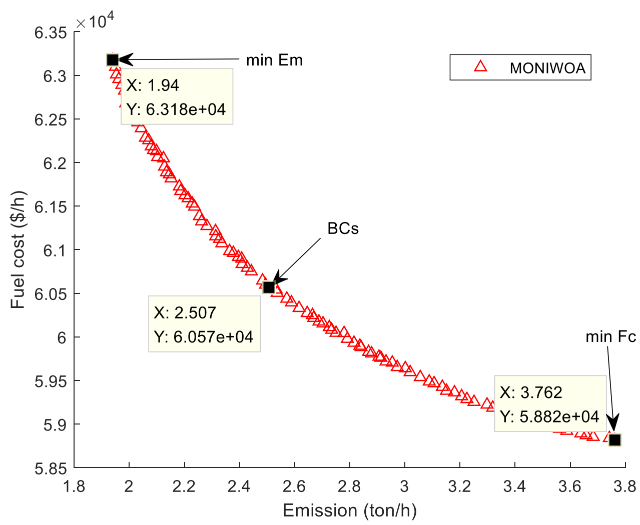

Fig. 24. The PFs of MONIWOA in CASE 8

three algorithms for CASE 1- CASE 8 are shown in TABLE XV. The more complicated the structure of power system is, the longer average running time is by using the same algorithm. Meanwhile, it can be clearly seen that the average running time of the MONIWOA algorithm is smaller than MODE and MOPSO algorithms. Therefore, the proposed algorithm has lower computation complexity.

Performance criteria has a significant role in evaluating the quality of the POS sets for the MOOPF problem. In order to verify the efficiency of the MONIWOA, MODE and MOPSO algorithms intuitively, *GD* and *SP* are adopted in this paper. The two different metrics of performance criteria are used to evaluate the distribution and convergence of the POS sets.

TABLE XIII
CONTROL VARIABLES OF BCS FOR CASE 7

control variables	MONIWOA	MODE	control variables	MONIWOA	MODE
P_{4}(MW)	11.0992	21.2278	V_{26}(p.u)	1.0301	1.0327
P_{6}(MW)	5.0000	11.4538	V_{27}(p.u)	1.0345	1.0087
P_{8}(MW)	5.0000	9.4703	V_{31}(p.u)	1.0258	1.0197
P_{10}(MW)	192.5740	230.0814	V_{32}(p.u)	1.0146	0.9852
P_{12}(MW)	175.4719	208.5465	V_{34}(p.u)	1.0107	0.9802
P_{15}(MW)	17.5566	20.6453	V_{36}(p.u)	0.9966	0.9998
P_{18}(MW)	36.9224	30.9857	V_{40}(p.u)	0.9858	1.0143
P_{19}(MW)	6.5167	8.1455	V_{42}(p.u)	1.0149	0.9868
P_{24}(MW)	10.2234	13.0185	V_{46}(p.u)	1.0404	1.0092
P_{25}(MW)	115.0520	113.8402	V_{49}(p.u)	1.0232	1.0127
P_{26}(MW)	350.0000	262.2970	V_{54}(p.u)	1.0142	1.0146
P_{27}(MW)	8.0000	8.5651	V_{55}(p.u)	1.0212	1.0125
P_{31}(MW)	8.0000	21.6234	V_{56}(p.u)	1.0420	0.9777
P_{32}(MW)	58.1022	38.2305	V_{59}(p.u)	1.0289	1.0034
P_{34}(MW)	16.5776	11.8665	V_{61}(p.u)	1.0255	1.0262
P_{36}(MW)	34.3270	59.6118	V_{62}(p.u)	1.0206	1.0186
P_{40}(MW)	8.9091	9.9605	V_{65}(p.u)	1.0268	1.01242
P_{42}(MW)	8.0000	25.6918	V_{66}(p.u)	1.0507	1.0397
P_{46}(MW)	55.5290	65.7009	V_{69}(p.u)	1.0351	1.0149
P_{49}(MW)	169.2688	176.7237	V_{70}(p.u)	1.0035	1.0488
P_{54}(MW)	193.4618	193.0659	V_{72}(p.u)	1.0416	0.9870
P_{55}(MW)	49.1474	35.6814	V_{73}(p.u)	1.0249	1.0168
P_{56}(MW)	25.0000	48.3199	V_{74}(p.u)	1.0008	0.9831
P_{59}(MW)	161.9553	50.1732	V_{76}(p.u)	1.0298	1.0156
P_{61}(MW)	121.5224	166.7341	V_{77}(p.u)	1.04727	1.0174
P_{62}(MW)	25.0000	59.7383	V_{80}(p.u)	1.02969	1.0125
P_{65}(MW)	266.2736	231.5880	V_{85}(p.u)	0.9875	0.9796
P_{66}(MW)	275.9027	292.4735	V_{87}(p.u)	0.9413	0.9608
P_{69}(MW)	67.8916	44.9405	V_{89}(p.u)	1.0329	1.0068
P_{70}(MW)	12.4386	10.0152	V_{90}(p.u)	0.9995	0.9509
P_{72}(MW)	13.4576	13.0250	V_{91}(p.u)	0.9958	0.9938
P_{73}(MW)	12.0199	5.0483	V_{92}(p.u)	1.0521	1.0007
P_{74}(MW)	34.1097	74.9481	V_{99}(p.u)	1.0676	0.9996
P_{76}(MW)	52.5534	28.0063	V_{100}(p.u)	1.0531	0.9967
P_{77}(MW)	174.8105	150.0390	V_{103}(p.u)	1.0432	1.0017
P_{80}(MW)	50.7584	34.9725	V_{104}(p.u)	1.0328	0.9847
P_{85}(MW)	10.0000	10.0278	V_{105}(p.u)	1.0385	0.9895
P_{87}(MW)	100.0000	112.3313	V_{107}(p.u)	1.0123	0.9590
P_{89}(MW)	91.7276	101.9808	V_{110}(p.u)	1.0297	1.0355
P_{90}(MW)	10.0273	9.3861	V_{111}(p.u)	1.0328	1.0541
P_{91}(MW)	20.8679	20.0043	V_{112}(p.u)	1.0103	1.0413
P_{92}(MW)	113.0012	118.1029	V_{113}(p.u)	1.0111	1.0060
P_{99}(MW)	119.0691	110.8054	V_{116}(p.u)	1.0338	1.0107
P_{100}(MW)	113.5530	124.1981	T_{8}(p.u)	0.9813	0.9990
P_{103}(MW)	8.8465	9.2071	T_{32}(p.u)	1.0105	1.0433
P_{104}(MW)	28.9389	25.0154	T_{36}(p.u)	1.0339	0.9182
P_{105}(MW)	52.4616	30.5751	T_{51}(p.u)	1.0042	0.9832
P_{107}(MW)	13.6336	8.0846	T_{93}(p.u)	0.9475	1.0235
P_{110}(MW)	32.2034	37.8142	T_{95}(p.u)	1.0686	1.0119
P_{111}(MW)	25.8114	28.6605	T_{102}(p.u)	0.9628	0.9784
P_{112}(MW)	51.2158	41.8487	T_{107}(p.u)	0.9640	0.9416
P_{113}(MW)	36.4916	32.7998	T_{127}(p.u)	0.9778	0.9391
P_{116}(MW)	37.1284	35.1674	Q_{34}(p.u)	0.1977	0.0414
V_{1}(p.u)	1.0443	1.0138	Q_{44}(p.u)	0.1085	0.1705
V_{4}(p.u)	1.0399	1.0419	Q_{45}(p.u)	0.1457	0.0702
V_{6}(p.u)	1.0133	1.0027	Q_{46}(p.u)	0.0162	0.0651
V_{8}(p.u)	1.0463	1.0641	Q_{48}(p.u)	0.2163	0.1750
V_{10}(p.u)	1.0286	1.0226	Q_{74}(p.u)	0.1127	0.1208
V_{12}(p.u)	0.9972	0.9875	Q_{79}(p.u)	0.1513	0.0642
V_{15}(p.u)	0.9989	0.9994	Q_{82}(p.u)	0.0000	0.0842
V_{18}(p.u)	1.0035	0.9994	Q_{83}(p.u)	0.1814	0.0319
V_{19}(p.u)	1.0384	1.0158	Q_{105}(p.u)	0.0866	0.1768
V_{24}(p.u)	1.0285	1.0040	Q_{107}(p.u)	0.1544	0.0065
V_{25}(p.u)	1.0432	1.0170	Q_{110}(p.u)	0.1612	0.0498
			Obj1 ($/h)	**58586.8759**	59433.2483
			Obj2(MW)	**56.1994**	58.1511

TABLE XIV
CONTROL VARIABLES OF BCS FOR CASE 8

control variables	MONIWOA	MODE	control variables	MONIWOA	MODE
P_{4}(MW)	5.0372	5.4778	V_{26}(p.u)	0.9745	1.0372
P_{6}(MW)	7.4956	9.8336	V_{27}(p.u)	1.0250	1.0026
P_{8}(MW)	5.9673	5.2622	V_{31}(p.u)	1.0131	1.0086
P_{10}(MW)	235.4062	221.7530	V_{32}(p.u)	1.0349	0.9920
P_{12}(MW)	182.4747	185.3345	V_{34}(p.u)	1.0234	0.9927
P_{15}(MW)	21.0675	20.2062	V_{36}(p.u)	1.0282	0.9871
P_{18}(MW)	69.8603	57.1962	V_{40}(p.u)	1.0189	0.9366
P_{19}(MW)	6.0096	5.43385	V_{42}(p.u)	1.0184	1.0360
P_{24}(MW)	10.6072	6.4226	V_{46}(p.u)	1.0093	1.0342
P_{25}(MW)	104.5857	101.0000	V_{49}(p.u)	1.0036	0.9970
P_{26}(MW)	100.0000	100.0000	V_{54}(p.u)	0.9918	1.0038
P_{27}(MW)	8.1538	23.3969	V_{55}(p.u)	0.9948	0.9834
P_{31}(MW)	19.8880	11.9824	V_{56}(p.u)	0.9891	0.9841
P_{32}(MW)	41.9303	98.5838	V_{59}(p.u)	1.0212	0.9990
P_{34}(MW)	14.4233	11.9148	V_{61}(p.u)	1.0008	0.9948
P_{36}(MW)	25.7039	25.0000	V_{62}(p.u)	1.0106	0.9860
P_{40}(MW)	9.0574	17.4710	V_{65}(p.u)	0.9859	1.0166
P_{42}(MW)	8.7728	13.0751	V_{66}(p.u)	1.02670	1.0310
P_{46}(MW)	36.5289	59.2273	V_{69}(p.u)	1.0108	1.0368
P_{49}(MW)	227.1384	222.3265	V_{70}(p.u)	1.0305	1.0157
P_{54}(MW)	129.5572	72.9188	V_{72}(p.u)	0.9673	1.0233
P_{55}(MW)	28.9941	31.5064	V_{73}(p.u)	0.9832	1.0411
P_{56}(MW)	39.2090	36.6307	V_{74}(p.u)	0.9638	0.9983
P_{59}(MW)	50.0000	52.0443	V_{76}(p.u)	1.0283	1.0293
P_{61}(MW)	117.1979	192.1330	V_{77}(p.u)	1.0313	1.0126
P_{62}(MW)	80.3951	69.9425	V_{80}(p.u)	1.0211	1.0065
P_{65}(MW)	420.0000	334.9753	V_{85}(p.u)	0.9770	1.0003
P_{66}(MW)	278.4056	173.1385	V_{87}(p.u)	0.9743	0.9816
P_{69}(MW)	30.8531	50.3196	V_{89}(p.u)	1.0320	0.9877
P_{70}(MW)	21.1261	20.4516	V_{90}(p.u)	1.0116	0.9909
P_{72}(MW)	6.3411	7.3582	V_{91}(p.u)	1.0101	1.0251
P_{73}(MW)	9.1643	11.0914	V_{92}(p.u)	1.0280	1.0278
P_{74}(MW)	26.1935	37.8101	V_{99}(p.u)	1.0328	1.0442
P_{76}(MW)	34.6505	45.3501	V_{100}(p.u)	1.0411	1.0199
P_{77}(MW)	213.3085	232.4308	V_{103}(p.u)	1.0098	1.0184
P_{80}(MW)	59.4893	37.3059	V_{104}(p.u)	1.0124	1.0426
P_{85}(MW)	21.4155	21.7041	V_{105}(p.u)	1.0053	1.0591
P_{87}(MW)	158.7767	201.2808	V_{107}(p.u)	0.9968	1.0193
P_{89}(MW)	73.1502	129.8749	V_{110}(p.u)	1.0180	0.9826
P_{90}(MW)	10.3102	9.8739	V_{111}(p.u)	1.0204	0.9661
P_{91}(MW)	29.3140	36.4363	V_{112}(p.u)	1.0191	0.9827
P_{92}(MW)	141.2528	108.9703	V_{113}(p.u)	1.0221	1.0554
P_{99}(MW)	123.2524	200.5219	V_{116}(p.u)	1.0613	1.0020
P_{100}(MW)	216.5197	151.0350	T_{8}(p.u)	0.9645	0.9956
P_{103}(MW)	11.54846	9.4878	T_{32}(p.u)	1.0017	0.9591
P_{104}(MW)	28.6152	40.2780	T_{36}(p.u)	0.9947	0.9927
P_{105}(MW)	28.2431	29.6691	T_{51}(p.u)	0.9409	0.9419
P_{107}(MW)	13.8267	8.0052	T_{93}(p.u)	0.9572	1.0350
P_{110}(MW)	33.3349	25.7384	T_{95}(p.u)	1.0133	1.0010
P_{111}(MW)	37.9122	42.9920	T_{102}(p.u)	0.9180	0.926
P_{112}(MW)	33.9259	65.8258	T_{107}(p.u)	0.9006	0.9336
P_{113}(MW)	58.2439	37.0346	T_{127}(p.u)	1.0231	1.0298
P_{116}(MW)	37.0737	42.1695	Q_{34}(p.u)	0.1363	0.2152
V_{1}(p.u)	1.0090	0.9902	Q_{44}(p.u)	0.0737	0.1365
V_{4}(p.u)	1.0312	1.0193	Q_{45}(p.u)	0.1317	0.0501
V_{6}(p.u)	0.9896	1.0215	Q_{46}(p.u)	0.2298	0.0323
V_{8}(p.u)	1.0388	0.9934	Q_{48}(p.u)	0.0450	0.3000
V_{10}(p.u)	0.9945	1.0201	Q_{74}(p.u)	0.2156	0.1641
V_{12}(p.u)	0.9843	0.9808	Q_{79}(p.u)	0.1937	0.1798
V_{15}(p.u)	1.0423	1.0172	Q_{82}(p.u)	0.1125	0.0572
V_{18}(p.u)	0.9767	1.0095	Q_{83}(p.u)	0.1597	0.2054
V_{19}(p.u)	1.0489	0.9809	Q_{105}(p.u)	0.2596	0.2396
V_{24}(p.u)	1.0513	1.0282	Q_{107}(p.u)	0.2736	0.0776
V_{25}(p.u)	0.9836	1.0091	Q_{110}(p.u)	0.0226	0.1743
			Obj1 ($/h)	**60567.8210**	60928.7800
			Obj2(MW)	**2.5066**	2.5886

1) GD

The *GD* factor is used to calculate the distance between PFs sets of MONIWOA method and the real PFs. The real PFs represents the best one among the obtained PFs solutions, and a value of *GD*=0 represents that all the candidate solutions are in line with the real PFs[29]. Consequently, the

TABLE XV
AVERAGE RUNNING TIME

Algorithm	CASE 1	CASE 2	CASE 3	CASE 4	CASE 5	CASE 6	CASE 7	CASE 8
MONIWOA	237.645	251.5658	259.5532	341.9074	384.11215	559.3032	1477.9135	1503.6842
MODE	239.9258	257.0107	264.2912	349.8874	402.2325	568.0086	1509.7569	1507.3793
MOPSO	241.8017	260.6698	362.916	350.61015	411.0507	564.2995		

TABLE XVI
THE RESULTS OF GD FOR MONIWOA, MODE, MOPSO ALGORITHMS

Indicator	Test CASE	MONIWOA		MODE		MOPSO	
		Mean	Deviation	Mean	Deviation	Mean	Deviation
GD	CASE 1	0.0654	0.0125	0.0710	0.0137	0.0841	0.0361
	CASE 2	0.0136	0.0048	0.0253	0.0062	0.0224	0.0118
	CASE 3	0.0580	0.0018	0.0757	0.0140	0.0878	0.0162
	CASE 4	0.0766	0.0034	0.0806	0.0094	0.0898	0.0183
	CASE 5	0.2548	0.0216	0.4084	0.1306	3.3276	1.3364
	CASE 6	0.4524	0.0884	0.4790	0.1359	0.5300	0.1250
	CASE 7	0.2554	0.0600	0.7745	0.3062		
	CASE 8	0.5060	0.2293	1.1839	0.6098		

TABLE XVII
THE RESULTS OF SP FOR MONIWOA, MODE, MOPSO ALGORITHMS

Indicator	Test CASE	MONIWOA		MODE		MOPSO	
		Mean	Deviation	Mean	Deviation	Mean	Deviation
SP	CASE 1	0.6822	0.0344	0.7323	0.0534	0.9691	0.0662
	CASE 2	0.0005	0.0003	0.0009	0.0012	0.0025	0.0007
	CASE 3	0.8997	0.0674	1.0154	0.0505	0.8979	0.2784
	CASE 4	1.0527	0.1089	1.2039	0.0967	0.8723	0.3115
	CASE 5	13.0477	2.2445	46.1916	23.3778	15.1420	8.0880
	CASE 6	28.8606	1.5797	46.5911	26.9392	95.1347	53.2685
	CASE 7	10.4228	2.4473	9.9762	3.3746		
	CASE 8	18.4330	2.2514	25.9783	15.6398		

smaller the *GD* is, the better convergence of the current obtained PFs solutions is to the real PFs. The *GD* can be expressed as follows:

$$GD = \frac{\sqrt{\sum_{j=1}^{m} dis_j^2}}{m} \tag{48}$$

where m indicates the total number of all the candidat solutions. dis_j represents the Euclidean distance between the PFs of *j*th solution and the real one.

2) *SP*

The SP factor is used to evaluate the uniformity of the optimal POS set through measuring the standard variance range of the adjacent candidate solutions, and a value of SP=0 represents that all the candidate solutions are evenly distributed. Consequently, the smaller the SP is, the better distribution uniformity of the current PFs is. The SP can be expressed as follows:

$$\begin{cases} SP = \sqrt{\dfrac{1}{Ns-1}\sum_{s=1}^{Ns}\left(\dfrac{1}{Ns}\sum_{s=1}^{Ns} d_s - d_s\right)^2} \\ d_s = \min_{t=1,2,\cdots Ns}\left(\sum_{k=1}^{M}\left|P_k^s - P_k^t\right|\right) \end{cases} \tag{49}$$

where Ns represents the total number of d_s.

3) Statistical analysis

Boxplot, a predominant tool to analyze the GD and HV, can display a intuitive comparison of the statistical data, which is obtained by the MONIWOA, MODE and MOPSO algorithms. Especially, we can evaluate convergence and stability through the comparison of the boxplot's maximum, minimum, median, outlier, upper quartile and lower quartile[29].

Boxplots of *GD* for CASE 1- CASE 8 are intuitively shown in Fig. 25. The MONIWOA algorithm has dominant ability to seek out smaller mean values and fewer outliers in all cases, and the results clearly demonstrates that the MONIWOA method is better than MODE and MOPSO algorithms, Therefore, it proves that the obtained PFs of MONIWOA method is more closer to the real PFs when compared with other algorithms.

Boxplots of *SP* for CASE 1- CASE 8 are intuitively shown in Fig. 26. As compared to MODE and MOPSO algorithms, it can be clearly seen that the MONIWOA method has competitive advantages to pick up smaller median value with fewer outlier. Obviously, the *SP* obtained by MONIWOA method have superior advantages to obtain better POS sets than other algorithms.

The mean and deviation of *GD* for CASE 1- CASE 8 are shown in TABLE XVI, and the mean and deviation of *SP* for CASE 1- CASE 8 are shown in TABLE XVII. It is worth noting that the novel MONIWOA algorithm has strong ability to obtain minimal values of mean and deviation for *GD* simultaneously in most cases, and it also can obtain minimal values of mean and deviation for *SP* simultaneously in most cases. Consequently, it clearly shows that the MONIWOA algorithm can obtain more uniform distribution and better convergence of PFs than MODE and MOPSO algorithms when dealing with the MOOPF problem in all cases.

4) Wilcoxon signed-rank test

Wilcoxon signed-rank test is chosen to evaluate the performance of the MONIWOA algorithm in different power systems through testing the null hypothesis. In CASE 1, The BCs of *Fc* and *Em* and comparison results are chosen to calculate by the Wilcoxon signed-rank test approach in the system1, and the outcomes are shown in TABLE XVIII. In CASE 7, The BCs of *Fc* and P_l and comparison results are

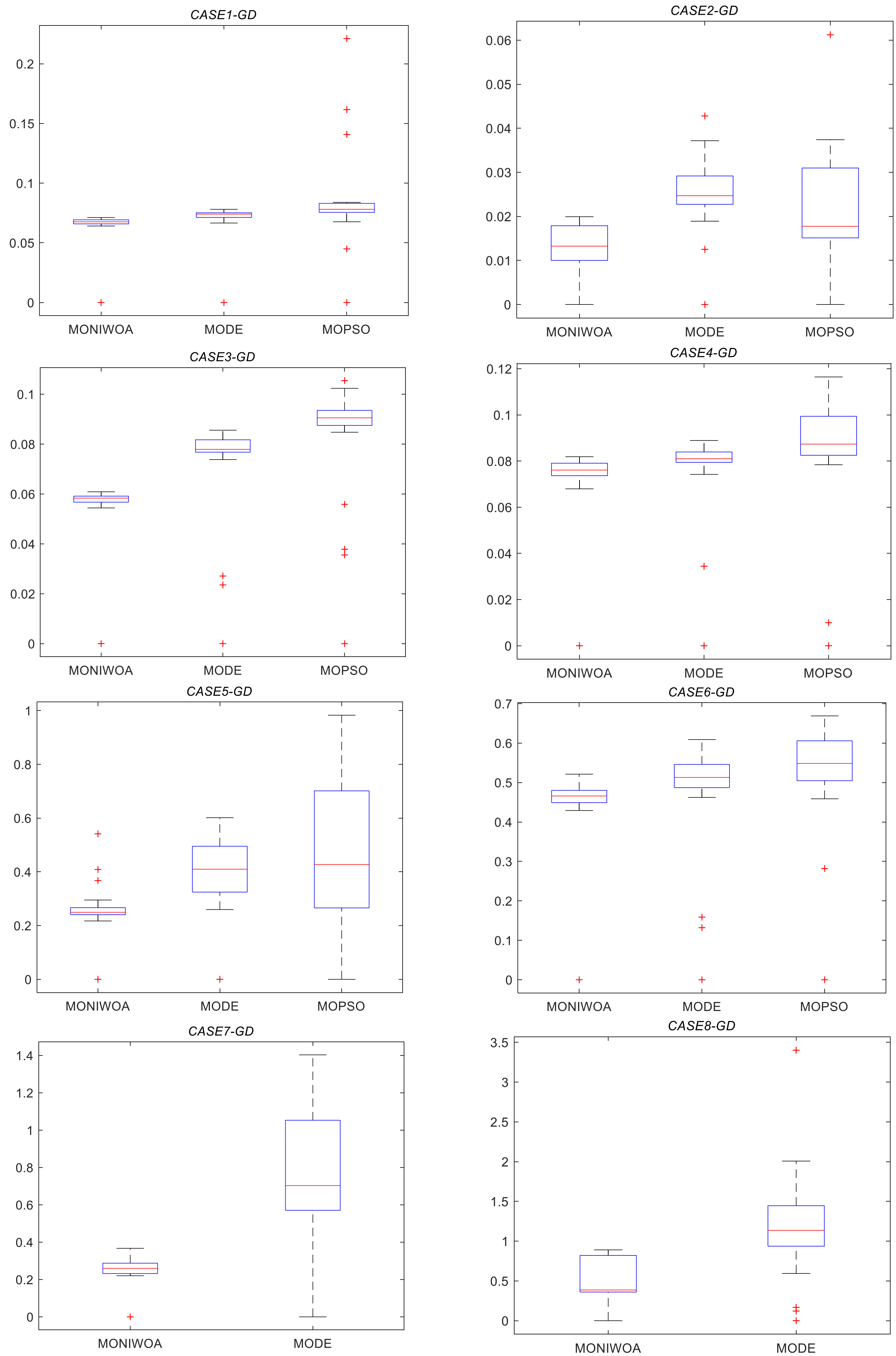

Fig. 25. Boxplots of *GD* for MONIWOA, MODE and MOPSO

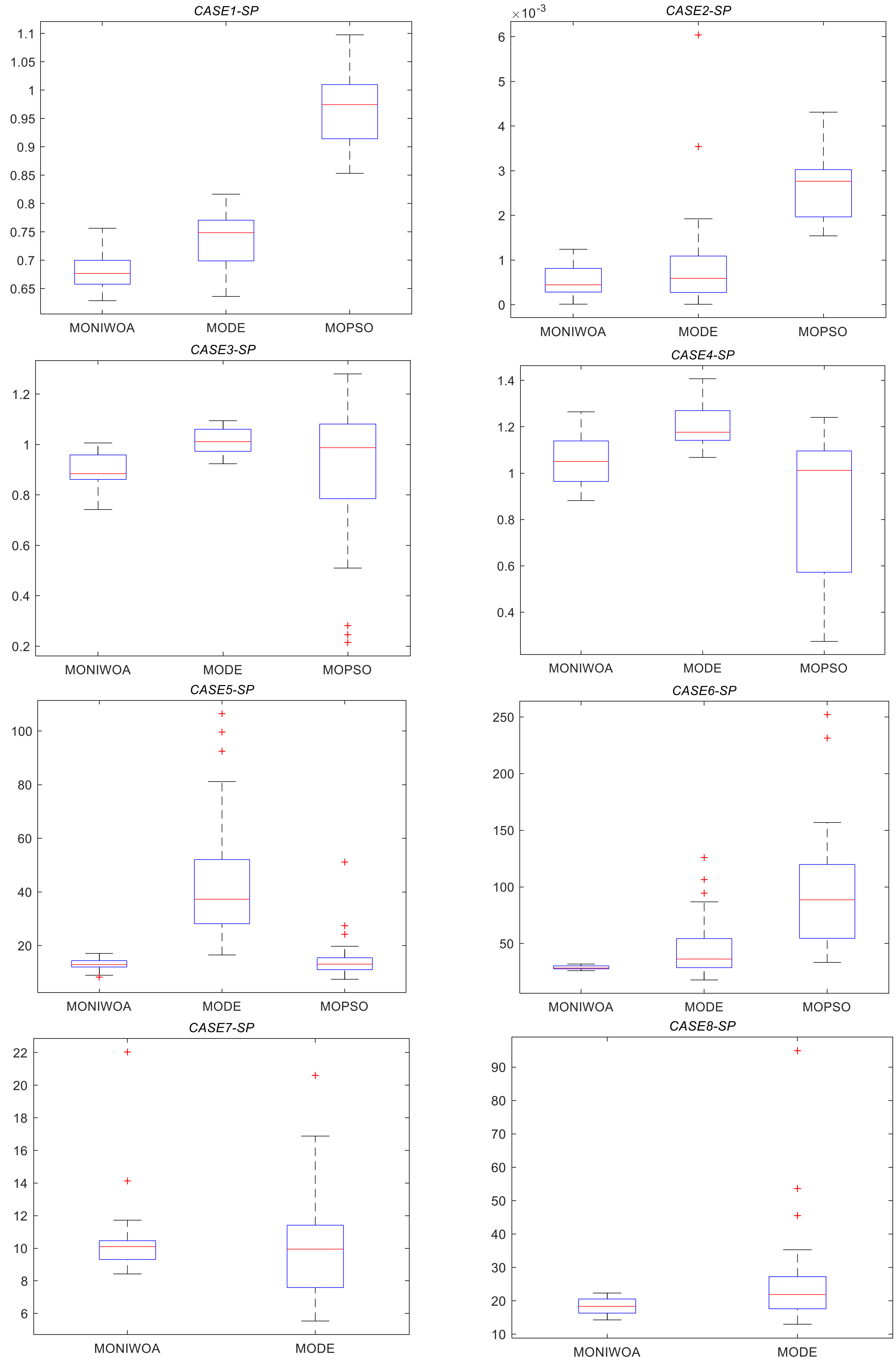

Fig. 26. Boxplots of SP for MONIWOA, MODE and MOPSO

chosen to calculate by the Wilcoxon signed-rank test approach in the system3, and the results are shown in TABLE XIX.

As is shown in TABLE XVIII, the values of p (p=0.0179 and 0.0179 in system1-CASE 1) are all obviously less than the significance level (α=0.05), so the MONIWOA algorithm has a competitive advantage over obtaining the more optimal BCs of *Fc* and *Em* as compared to other algorithms in system1. As is shown in TABLE XIX, the values of p (p=0.0431 and 0.431 in system3-CASE 7) are less than the significance level (α=0.05), and the results demonstrates that the MONIWOA algorithm has a considerable advantage over obtaining the optimal BCs of *Fc* and P_l as compared to other algorithms in a more complicated power system.

TABLE XVIII

WILCOXON TEST OUTCOMES OF SYSTEM1 - CASE 1(REF=MONIWOA(*Fc* =**834.1110**, *Em* =**0.2311**))

Algorithm	*Fc* ($/h)	T	*Em* (ton/h)	T
MOPSO	836.2408	+	0.2489	+
MODE	834.9988	+	0.2431	+
NSGA-II [1]	837.7028	+	0.2434	+
NSGA-III [23]	836.4405	+	0.2423	+
PSO [32]	883.2800	+	0.2388	+
GSO [32]	852.8900	+	0.2446	+
ASGO [33]	843.5473	+	0.2539	+
		R^+=28.0000 R^-=0.00000		R^+=28.0000 R^-=0.0000
		p=0.0179		p=0.0179

TABLE XIX

WILCOXON TEST OUTCOMES OF SYSTEM3 - CASE 7(REF=MONIWOA(*Fc* =**58586.8759**, P_l =**56.1994**))

Algorithm	*Fc* ($/h)	T	P_l (MW)	T
MODE	59433.2483	+	58.1511	+
NSGA-II [30]	59900.3741	+	58.8192	+
NSGA-III [20]	59474.4030	+	58.4603	+
HFBA-COFS [30]	59624.0613	+	61.0362	+
MOPSO [20]	59133.1054	+	57.0368	+
		R^+=15.0000 R^-=0.0000		R^+=15.0000 R^-=0.0000
		p=0.0431		p=0.0431

V. CONCLUSION

In this paper, the standard WOA algorithm has some drawbacks with respect to the research of non-convex MOOPF problem. Here, some improved strategies which include piecewise non-linear strategy, dual dynamic weights mode and Lévy flight mechanism are employed to improve the performance of the WOA. Additionally, CPDR rule and CDRS strategy are adopted to deal with the MOOPF problem. In order to verify the effectiveness of the improved strategies, eight experiments which includes seven bi-objective functions and one tri-objective functions are tested in IEEE 30-bus, 57-bus and 118-bus systems. In CASE 1- CASE 8, all the objective functions of the BCs obtained by MONIWOA approach are smaller than the ones of MODE and MOPSO algorithms correspondingly, and the MONIWOA's average running time is smaller than others. In CASE 1 and CASE 7, it is clearly seen that the MONIWOA approach can find smaller objective functions of the BCs when compared with the results of other reported algorithms. High-quality POS and ideal BCs solutions obtained by MONIWOA approach prove that the novel approach owns outstanding superiority.

In addition, the results of *GD* and *SP* factors prove that the MONWOA approach has better ability of obtaining highly-convergent and evenly-distributed PFs than MODE and MOPSO algorithms. In summary, it can be concluded that the MONIWOA approach can tackle the complicated MOOPF problem more effectively.

REFERENCES

[1] G. Chen, X. Yi, Z. Zhang and H. Wang, "Applications of multi-objective dimension-based firefly algorithm to optimize the power losses, emission, and cost in power systems," *Applied Soft Computing*, vol. 68, pp. 322-342, 2018.

[2] G. Chen, Z. Lu and Z. Zhang, "Improved Krill Herd Algorithm with Novel Constraint Handling Method for Solving Optimal Power Flow Problems," *Energies*, vol. 11, no. 1, pp. 76-102, 2018.

[3] M. A. M. Shaheen, H. M. Hasanien and A. Al-Durra, "Solving of Optimal Power Flow Problem Including Renewable Energy Resources Using HEAP Optimization Algorithm," *IEEE Access*, vol. 9, pp. 35846-35863, 2021.

[4] S. Rahmani and N. Amjady, "Improved normalised normal constraint method to solve multi-objective optimal power flow problem," *IET Generation, Transmission and Distribution*, vol. 12, no. 4, pp. 859-872, 2018.

[5] G. Chen, J. Cao, Z. Zhang and Z. Sun, "Application of Imperialist Competitive Algorithm with its Enhanced Approaches for Multi-objective Optimal Reactive Power Dispatch Problem," *Engineering Letters*, vol. 27, no. 3, pp. 579-592, 2019.

[6] J. Zhang, Q. Tang, P. Li, D. Deng and Y. Chen, "A modified MOEA/D approach to the solution of multi-objective optimal power flow problem," *Applied Soft Computing*, vol. 47, pp. 494-514, 2016.

[7] A. Khan, H. Hizam, N. I. Abdul-Wahab and M. L. Othman, "Solution of Optimal Power Flow Using Non-dominated Sorting Multi Objective Based Hybrid Firefly and Particle Swarm Optimization Algorithm," *Energies*, vol. 13, no. 16, pp. 4265-4288, 2020.

[8] M. Ghasemi, S. Ghavidel, M. M. Ghanbarian and M. Gitizadeh, "Multi-objective optimal electric power planning in the power system using gaussian bare-bones imperialist competitive algorithm," *Information Sciences*, vol. 294, pp. 286-304, 2015.

[9] E. Naderi, M. Pourakbari-Kasmaei, F. V. Cerna and M. Lehtonen, "A novel hybrid self-adaptive heuristic algorithm to handle single- and multi-objective optimal power flow problems," *International Journal of Electrical Power & Energy Systems*, vol. 125, pp. 106492-106508, 2021.

[10] G. Chen, J. Qian, Z. Zhang and S. Li, "Application of modified

pigeon-inspired optimization algorithm and constraint-objective sorting rule on multi-objective optimal power flow problem," *Applied Soft Computing*, vol. 92, pp. 106321-106340, 2020.
[11] P. P. Biswas, P. N. Suganthan, R. Mallipeddi and G. A. J. Amaratunga, "Multi-objective optimal power flow solutions using a constraint handling technique of evolutionary algorithms," *Soft Computing*, vol. 24, no. 4, pp. 2999-3023, 2020.
[12] K. Abaci and V. Yamacli, "Differential search algorithm for solving multi-objective optimal power flow problem," *International Journal of Electrical Power & Energy Systems*, vol. 79, pp. 1-10, 2016.
[13] S. Mirjalili and A. Lewis, "The whale optimization algorithm," *Advances in Engineering Software*, vol. 95, pp. 51-67, 2016.
[14] J. Wang, P. Du, T. Niu and W. Yang, "A novel hybrid system based on a new proposed algorithm — multi-objective whale optimization algorithm for wind speed forecasting," *Applied Energy*, vol. 208, pp. 344-360, 2017.
[15] M. Abdel-Basset, G. Manogaran, D. El-Shahat and S. Mirjalili, "Integrating the whale algorithm with tabu search for quadratic assignment problem: a new approach for locating hospital departments," *Applied Soft Computing*, vol. 73, pp. 530-546, 2018.
[16] M. M. Mafarja and S. Mirjalili, "Hybrid whale optimization algorithm with simulated annealing for feature selection," *Neurocomputing*, vol. 260, pp. 302-312, 2017.
[17] A. N. Jadhav and N. Gomathi, "WGC: Hybridization of exponential grey wolf optimizer with whale optimization for data clustering," *Alexandria Engineering Journal*, vol. 57, no. 3, pp. 1569-1584, 2018.
[18] G. Chen, X. Man, Y. Long and Z. Zhang, "Application of Multi-objective New Whale Optimization Algorithm for Environment Economic Power Dispatch Problem," *Engineering Letters*, vol. 29, no. 1, pp. 68-81, 2021.
[19] M. A. E. Aziz, A. A. Ewees and A. E. Hassanien, "Whale Optimization Algorithm and Moth-Flame Optimization for multilevel thresholding image segmentation," *Expert Systems with Applications*, vol. 83, pp. 242-256, 2017.
[20] K. B. O. Medani, S. Sayah and A. Bekrar, "Whale optimization algorithm based optimal reactive power dispatch: A case study of the Algerian power system," *Electric Power Systems Research*, vol. 163, pp. 696-705, 2018.
[21] G. Chen, Y. Han, Z. Zhang, X. Zeng and S. Li, "Research on Multi-objective Active Power Optimization Simulation of Novel Improved Water Cycle Algorithm," *IAENG International Journal of Applied Mathematics*, vol. 51, no. 1, pp. 250-263, 2021.
[22] S. Sivasubramani and K. S. Swarup, "Multi-objective harmony search algorithm for optimal power flow problem," *International Journal of Electrical Power & Energy Systems*, vol. 33, no. 3, pp. 745-752, 2011.
[23] G. Chen, J. Qian, Z. Zhang and Z. Sun, "Applications of Novel Hybrid Bat Algorithm With Constrained Pareto Fuzzy Dominant Rule on Multi-Objective Optimal Power Flow Problems," *IEEE Access*, vol. 7, pp. 52060-52084, 2019.
[24] K. Deb, A. Pratap, S. Agarwal and T. Meyarivan, "A Fast and Elitist Multiobjective Genetic Algorithm: NSGA-II," *IEEE Transactions on Evolutionary Computation*, vol. 6, no. 2, pp. 182-197, 2002.
[25] K. Deb and H. Jain, "An Evolutionary Many-Objective Optimization Algorithm Using Reference-point Based Nondominated Sorting Approach, Part I: Solving Problems with Box Constraints," *IEEE Transactions on Evolutionary Computation*, vol. 18, no. 4, pp. 577-601, 2014.
[26] S. Li and J. Wang, "Improved Cuckoo Search Algorithm with Novel Searching Mechanism for Solving Unconstrained Function Optimization Problem," *IAENG International Journal of Computer Science*, vol. 44, no. 1, pp. 8-12, 2017.
[27] C. Charin, D. Ishak, M. A. A. M. Zainuri, B. Ismail and M. K. M. Jamil, "A hybrid of bio-inspired algorithm based on levy flight and particle swarm optimizations for photovoltaic system under partial shading conditions," *Solar Energy*, vol. 217, pp. 1-14, 2021.
[28] M. R. Narimani, R. Azizipanah-Abarghooee, B. Zoghdar-Moghadam-Shahrekohne and K. Gholami, "A novel approach to multi-objective optimal power flow by a new hybrid optimization algorithm considering generator constraints and multi-fuel type," *Energy*, vol. 49, pp. 119-136, 2013.
[29] G. Chen, J. Qian, Z. Zhang and Z. Sun, "Multi-objective Improved Bat Algorithm for Optimizing Fuel cost, Emission and Active Power Loss in Power System," *IAENG International Journal of Computer Science*, vol. 46, no. 1, pp. 118-133, 2019.
[30] T. Ding, C. Li, F. Li, T. Chen and R. Liu, "A bi-objective DC-optimal power flow model using linear relaxation-based second order cone programming and its Pareto Frontier," *International Journal of Electrical Power & Energy Systems*, vol. 88, pp. 13-20, 2017.
[31] B. Mandal and P. K. Roy, "Multi-objective optimal power flow using quasi-oppositional teaching learning based optimization," *Applied Soft Computing Journal*, vol. 21, pp. 590-606, 2014.
[32] S. S. Reddy and C. S. Rathnam, "Optimal Power Flow using Glowworm Swarm Optimization," *International Journal of Electrical Power & Energy Systems*, vol. 80, pp. 128-139, 2016.
[33] N. Daryani, M. T. Hagh and S. Teimourzadeh, "Adaptive group search optimization algorithm for multi-objective optimal power flow problem," *Applied Soft Computing Journal*, vol. 38, pp. 1012-1024, 2016.
[34] G. Chen, J. Qian, Z. Zhang and Z. Sun, "Multi-Objective Optimal Power Flow Based on Hybrid Firefly-Bat Algorithm and Constraints-prior Object-fuzzy Sorting Strategy," *IEEE Access*, vol. 7, pp. 139726-139745, 2019.